INTERNATIONAL JOURNAL OF HYDROPOWER AND CIVIL ENGINEERING

E-ISSN: 2707-8310
P-ISSN: 2707-8302
Journal's Website
IJHCE 2025; 6(1): 25-47
Received: 05-03-2025
Accepted: 12-04-2025

Er. Shrawan Kumar Neupane
School of Engineering, Faculty of Science and Technology, Pokhara University, Pokhara, Nepal

RK Regmi
Department of Civil Engineering, Pulchowk Campus, Institute of Engineering, Tribhuvan University, Nepal

Er Shankar Lamichhane
School of Engineering, Faculty of Science and Technology, Pokhara University, Pokhara, Nepal

Corresponding Author:
Er. Shrawan Kumar Neupane
School of Engineering, Faculty of Science and Technology, Pokhara University, Pokhara, Nepal

Optimization of the size of stilling basin: A case study of fewa hydroelectric project

Er Shrawan Kumar Neupane, RK Regmi and Er Shankar Lamichhane

DOI: https://www.doi.org/10.22271/27078302.2025.v6.i1a.61

Abstract
This study explores advanced design modification strategies to enhance stilling basin performance, focusing on energy dissipation, flow depth, and depth-averaged velocity across eight numerical models. This research involves both numerical as well as iterative method during the study. Overall 8 different Model were created, each model unique with different shape and placing of the basin appurtenances. After running the simulations and post-processing, Model 2, incorporating honeycomb baffle blocks, demonstrated the highest efficiency with 11.8% reduction in basin length. Model 3 followed closely, with notable performance at a 7.2% length reduction. Models 4, 6, and 8 showed promising results with a 5% length reduction, while Model 5 and Model 7 exceeded acceptable hydraulic limits that was considered even earlier. The honeycomb structures proved effective due to their labyrinthine configuration, which induced turbulence and dispersion, thereby enhancing energy dissipation. Furthermore, they facilitated basin size optimization, critical in spatially constrained environments. Fundamentally, the use of honeycomb baffle blocks appears as a powerful method for enhancing energy dissipation and optimizing stilling basin size. These results warrant more investigation into the use of honeycomb structures in hydraulic engineering.

Keywords: Honeycomb structures, CFD, hydraulic modeling, flow3D hydro, stilling basin

Introduction
Hydropower remains a cornerstone of renewable energy development, particularly in countries with abundant water resources like Nepal. One of the critical challenges in hydropower systems is the safe and efficient dissipation of surplus kinetic energy from high-velocity flows released from spillways or outlets. This is essential to prevent downstream erosion, protect hydraulic structures, and ensure environmental stability. Stilling basins are widely used energy dissipation structures that facilitate the formation of hydraulic jumps, converting excess kinetic energy into turbulence and heat. The performance of a stilling basin heavily depends on the geometry and configuration of its appurtenances, structures such as baffle blocks, end sills, and chute blocks that promote turbulence and enhance energy dissipation. With the advent of advanced computational tools, Computational Fluid Dynamics (CFD) has emerged as a powerful method for simulating and optimizing hydraulic structures with high accuracy and flexibility.

This study focuses on the optimization of stilling basin design through the analysis of different appurtenance shapes, specifically curved blocks, triangular blocks, and honeycomb blocks. The objective is to evaluate and compare their performance in terms of energy dissipation efficiency, flow stabilization, and reduction in downstream scour potential. The Flow3D Hydro software is used as the simulation platform due to its proven capability of solving free-surface flows and complex turbulence interactions.

A case study of the Fewa Hydroelectric Project, located in Pokhara, Nepal, is used to contextualize the analysis. The original stilling basin configuration is taken as a baseline model, against which the alternative block geometries are assessed. The study aims to provide recommendations for more effective stilling basin configurations based on CFD simulation results, which could contribute to safer and more efficient hydropower development.

Research Objective
This research aims to study the total energy dissipation and compare the efficiency of various basin appurtenances, including curved, triangular, and honeycomb structures,

with the regular types recommended by the USBR. By conducting simulations using Flow3D Hydro and analyzing the results, the research will determine the most efficient shape for energy dissipation. These findings will contribute to the optimization of stilling basin design and enhance its hydraulic performance.

3. Methodology

The study utilizes a combination of field data collection, advanced modeling techniques, and simulation software (i.e., Flow3D Hydro) to capture the complex hydraulic phenomena occurring within the stilling basin. In addition, this methodology ensures accurate representation of the hydraulic conditions, facilitating a detailed analysis of the flow characteristics and energy dissipation performance.

Moreover, modification of each type of the model, within a predefined range (i.e. up to chute blocks), multiple simulations were conducted to evaluate the impact of different lengths on defined hydraulic parameters with the goal to optimize length with expected energy dissipation ensuring efficient operation of the stilling basin. This iterative optimization process, combined with thorough performance evaluation, allowed for the derivation of expected recommendations for the design and construction of an efficient stilling basin.

A Flowchart for the representation of the procedure of methodology was prepared before carrying out the study and analysis process, so that, the similar studies could be done, if required in the future regarding the stilling basin.

The methodology comprises of the following steps that were undertaken during the studies:

3.1 Site selection and Data Acquisition

The site selection process plays a crucial role in ensuring the accuracy and relevance of the study. At the outset, a thorough assessment of potential sites for the stilling basin at Fewa Hydroelectric project was conducted. Factors such as the proximity to the dam, accessibility, topography, and the availability of suitable hydraulic structures were taken into consideration. Stilling basin at Fewa Hydroelectric Project was selected for the study as the stilling basin contains basin appurtenances such as chute blocks and basin blocks.

The collection of hydraulic data involved detailed surveys and measurements conducted at the site. Parameters such as the dimensions of the stilling basin, chute blocks, baffle blocks, height of dam and water level were measured using appropriate instruments and techniques. In addition, hydraulic data, hydrological data was obtained from reliable sources, such as the Department of Hydrology and Meteorology (DHM). These data included historical flow records, precipitation data, and other hydrological parameters. The integration of hydrological data with the hydraulic data allowed for a comprehensive understanding of the inflow conditions and the potential variations in flow regimes.

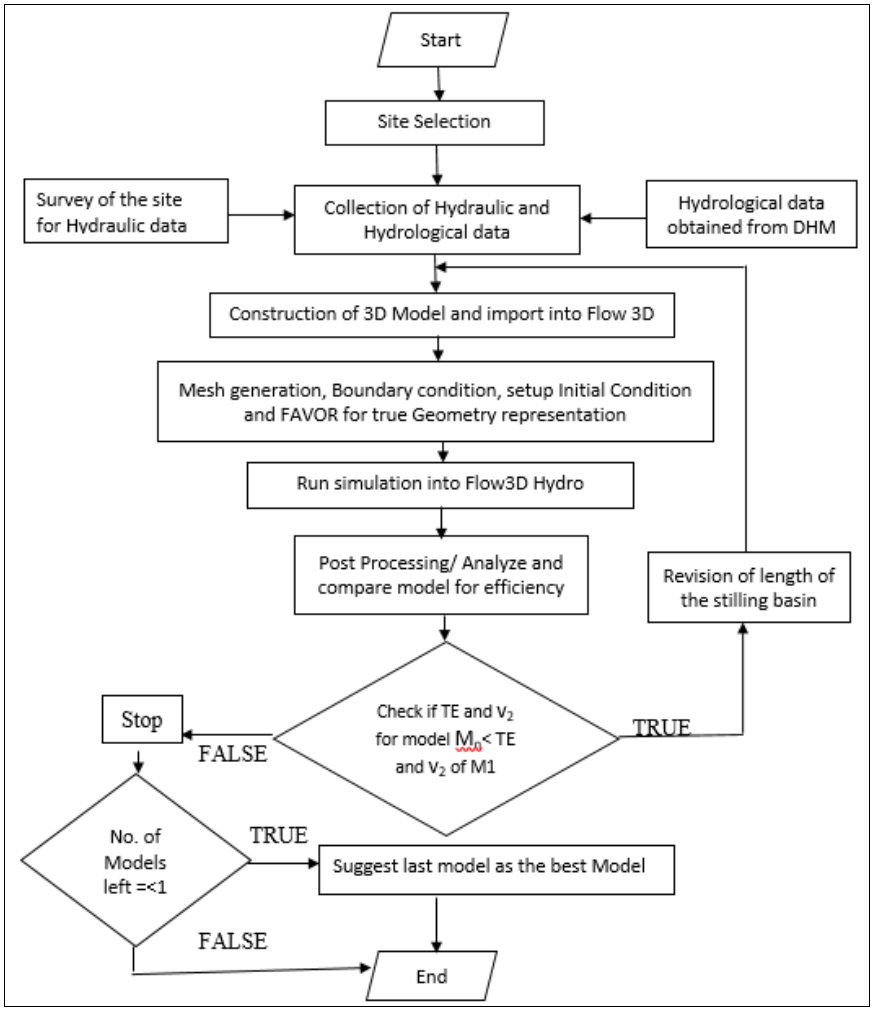

Fig 1: Flow chart for the process of work performed.

3.2 Numerical Modeling

Model Description

Each of the models were exported to Flow-3D Hydro in stl format, as Flow 3D Hydro consists of predefined characteristics of water that is capable of solving CFD problems relating fluid and hydraulic structures. 3D models after importing to the Flow3D Hydro, units of measurement were changed to SI and Physics was defined after that, including the RNG model that is capable of solving the turbulent flow. Also, fluid properties, mesh properties, boundary conditions such as water elevation, stagnation pressure, friction, etc. were assigned.

Furthermore, the limiters (i.e. water) were assigned, with Global and Region specific initial conditions in the model, after that the flux surface was defined and the model was ready to run and processing was begun. Analysis and Rendering were done after the completion of processing. Various hydraulic parameters such as velocity magnitude of the flow, flow depth, total hydraulic head and Froude number were obtained after the simulation was completed in every time frame that was defined.

Similarly, the models with the use of each types of blocks were made and simulated in the Flow3D Hydro. Later on, the analysis was done from the results obtained after completion of the simulation.

The total energy from upstream is extremely hard to cease, however, it can be reduced to the desired amount so that the devastating effects of the flow is avoided.

3.2.1 Construction of 3D Model

To construct the 3D model, the acquired site data were utilized in the AutoCAD software to plot the necessary dimensions and features accurately. The AutoCAD file was then exported to SketchUp, where the final 3D model was created. The model was meticulously designed to replicate the actual site conditions, ensuring its fidelity to the physical structure.

In the 3D model, the existing chute blocks and baffle blocks were replaced with alternative block configurations proposed for optimization. These new block types were carefully chosen based on their potential to enhance energy dissipation and improve hydraulic performance within the stilling basin.

The length of the stilling basin was set to begin at a distance of 8.29 meters from the origin, which corresponds to the back face of the dam. The basin width was determined as 28 meters, providing an adequate channel width for effective flow regulation. Additionally, the end sill height was specified as 0.83 meters, consisting of square blocks measuring 2 m * 2 m * 0.2 m. These blocks were arranged in three rows perpendicular to the flow direction, strategically positioned to influence the hydraulic behavior within the basin. To simulate and analyze the constructed 3D model, Flow3D Hydro software was employed.

3.2.2 Simulation Setup

The imported model from the SketchUp, was defined in the Flow3D Hydro by assigning different factors such as the mesh and physics, the further processes involved while working are as follows:

Defining the mesh of the appropriate size plays an important role in the output of the simulation and further analysis. To improve the output and save time, mesh size of 0.15 m was defined in the region containing the basin appurtenance and it was varied upto 2 m in the upstream where the flow does not need much analysis. Large mesh size was defined where there is least requirement of the analysis of the flow characteristics as well as the least rate of change in the geometry of the model. Mesh divided into varying size in each parts as per requirement has been shown in the figure alongside, Fig 2.

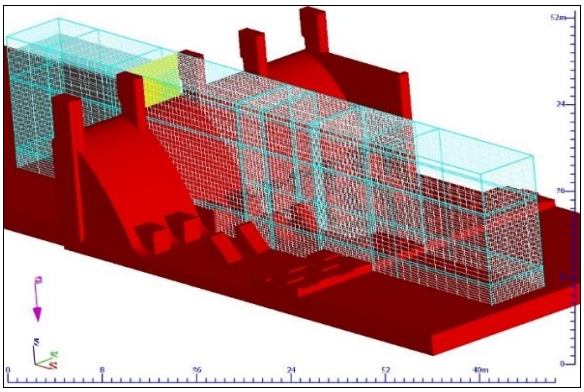

Fig 2: Mesh defined at various locations

The second step after defining the mesh is defining the physics. Afterwards fluid was defined, it is also predefined in the Flow3D Hydro, and the flow type was selected as RNG model.

The boundary conditions such as the floor, pressure and wall were defined afterwards in all the three axis. It includes the possible flow of the fluid, the pressure and possible conditions of the forces that is capable to affect the analysis and output. Here, in this model, upstream boundary condition is defined by the VOF and the downstream as the floor bottom as wall and fraction of the fluid set as zero that allows splashing of the fluid.

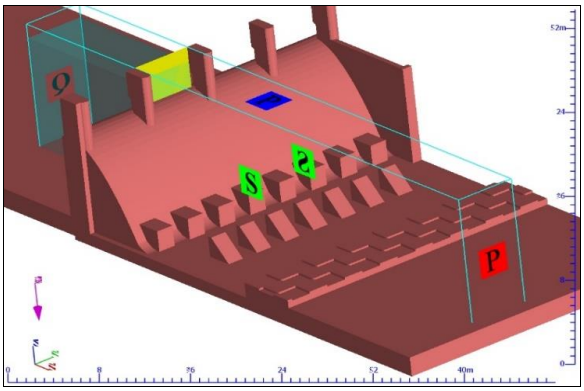

Fig 3: Setting up of Boundary Condition, view: 1

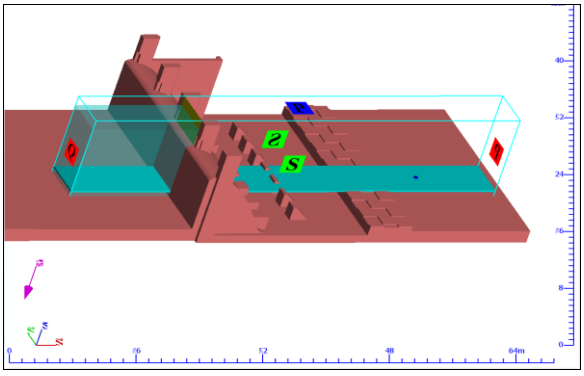

Fig 4: Setting up of Boundary Condition, view: 2

The notations for the boundary condition are Q, S and P, where, Q is discharge, S is Symmetry and P is Pressure. These notations can be seen on the considered boundary surface as defined.

The Initial condition of the fluid was defined with the Global and Regions, where, the Global condition defines the presence of water in all the selected area in Global initial condition. Similarly, Region was defined to set the water in the upstream portion of the Dam. Here, in this study, the Global initial condition was set for 0.83 m from bottom and Region was set to 11.5 m from the floor, fluid elevation as a stagnation pressure.

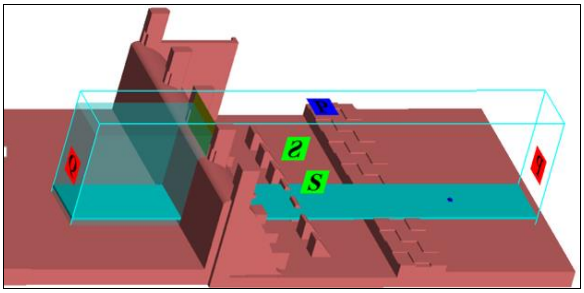

Fig 5: Setting Initial Condition of the fluid at U/S and D/S

Though the level of water was set at the elevation of 11.5 m, the U/S region was defined as the volume of flow with the discharge of 588.44 cumecs. As it can be seen in the figure above, a strip of the region has been taken for reducing the simulation time, the defined Q'= 147.11 cumecs. It is because, the flow through only one of the gate shall be Q'= Q/N, where N= number of gates= 4. The notation Q can be clearly seen in the figure above. After the construction of the model, it was FAVORized (Fractional Area Volume Obstacle Representation). It helps to visualize the shape of the solid structure and check for any distortion of the shapes. Hence, in the model, varying size of the mesh was defined at various locations of the model as the assumption in our case is that, the flow characteristics is defined by the shape of the blocks used in the stilling basin.

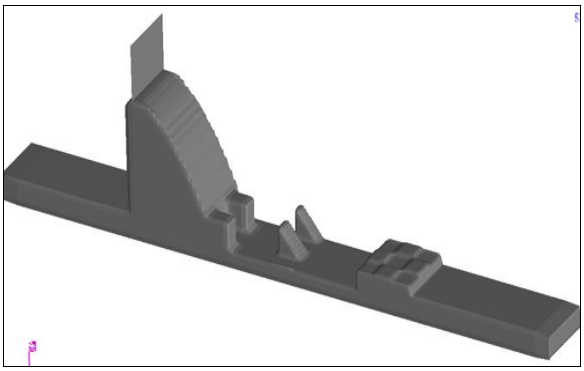

Fig: Model 1 after running FAVOR

The model was run after assigning all data, limiters (i.e. fluid) and boundary conditions.

1. Data were extracted from the analysis tab of the model. The data was further analyzed for the expected results.
2. All the steps were repeated for each of the model and, the trials were done varying the length of the stilling basin by shifting the end sill. The length was reduced by 2.5% of the length of the stilling basin and then by 5%, 7.5% and so on upto 12% to compare the results with Model1.

3.2.3 Description of the Models

All dimensions for each model were same like that of Model 1, whereas, the chute blocks and baffle blocks that are proposed were changed for each models, it gives the efficiency of the stilling basin for that model. The discharge was kept constant to 588.44 m^3/s, a 1000-year flood discharge, considered as design discharge for the stilling basin. Furthermore, iterative trials were done by reducing the length for each models by 2.5% for each trial, proceeding up to 11.8% of the length. The characteristics of each models that were run are described below:

Model 1: Model confirming to USBR III and Fewa Hydroelectric Project

Model 1 aimed to accurately represent the field conditions of the Fewa Hydroelectric Project site, ensuring that all dimensions and features of the stilling basin and its appurtenances were identical to those observed on-site. The dimensions of the stilling basin in this model were precisely replicated based on the field measurements. The dimension of the basin was L (length) = 21.23 meters, B (width) = 28 meters, and D (depth) = 1.57 meters. The baffle blocks had dimensions of L = 2.57 meters, B = 2.15 meters, and W = 1.61 meters.

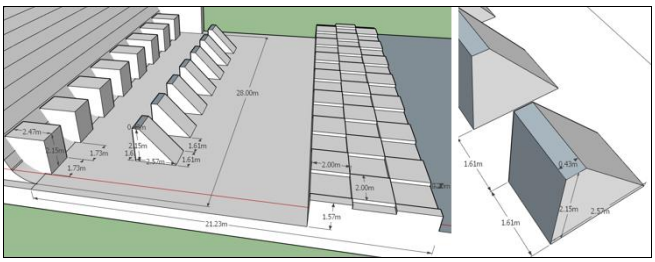

Fig 3.4. 2: 3D Model M_1 with regular USBR type stilling basin of Fewa Hydroelectric Project as per site

Model 2: Model with honeycomb basin blocks

Model 2, aimed at evaluating the performance of a honeycomb basin structure, involved replacing the basin blocks of Model 1 with a honeycomb configuration. In this configuration, rectangular blocks measuring 2.15 m * 2.15 m * 2.15 m were utilized. These blocks featured slots in a cylindrical shape with a diameter of 1.42 meters. Additionally, a central part of each block was sliced/deducted by a sphere with a diameter of 2.03 meters. While the basin blocks were modified in Model 2, the chute blocks were kept unchanged. This allowed for a comparative analysis between the two models, specifically assessing the impact of the honeycomb structure as baffle blocks on energy dissipation and hydraulic performance.

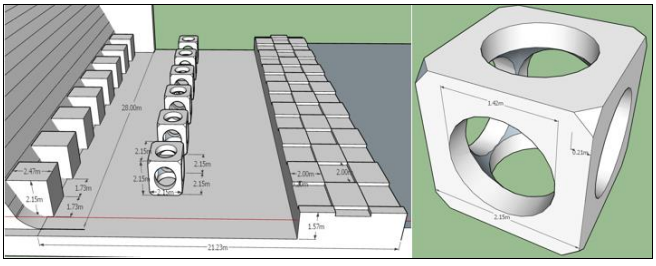

Figure 3.4. 3: 3D Model M_2 with honeycomb basin blocks.

Model 3: Model with curved (on horizontal surface) blocks as basin blocks and chute blocks. The curved blocks in this model were designed to have a distinct shape, with horizontal surfaces cut in a curved manner by a cylindrical surface with a diameter of 1.65 meters. This design alteration aimed to increase eddies in the flow and increase energy losses. The dimensions of each block = 2.15 m length, 2.15 m width, and 2.15 m height. The top width of the block was 1.07 meters, and the side view of the curved block showcased a trapezoidal shape, with a width of 2.15 meters at the bottom and a reduced width of 1.07 meters at the top.

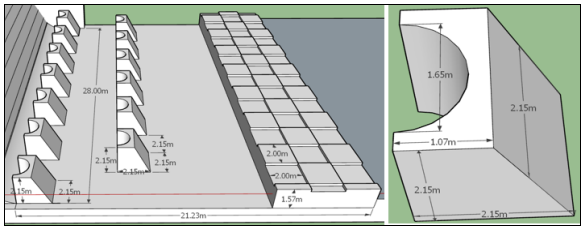

Fig 3.4. 4: Model M_3 with curved (on horizontal surface) basin blocks and curved chute blocks.

Model 4: Model with curved shape (on vertical surface) basin blocks and chute blocks.
In Model 4, the design of the stilling basin underwent modification of Model 1 by replacing the conventional chute blocks (i.e. recommended by USBR) and basin blocks with curved blocks that were cut on the vertical surface. Each curved block in this Model has dimensions of 2.15 meters in width, 2.15 meters in height, and 2.15 meters in length at the bottom. The length of the block reduced to 1.08 meters at the top.

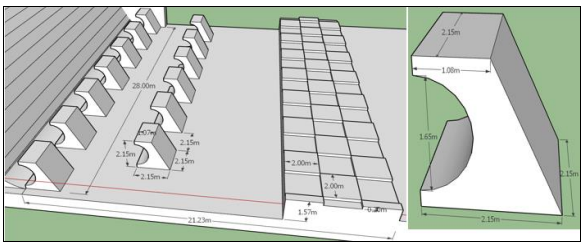

Fig 3.4. 5: Model M_4 with curved (on vertical surface) basin and chute blocks.

Model 5: Model with triangular basin blocks and chute blocks.
The triangular blocks in Model 5 had dimensions of 2.15 meters for each face, forming an equilateral triangle. The height of the triangular blocks from the plan view was also 2.15 meters. This triangular shape was chosen to explore its impact on flow control, turbulence reduction, and energy dissipation within the stilling basin.

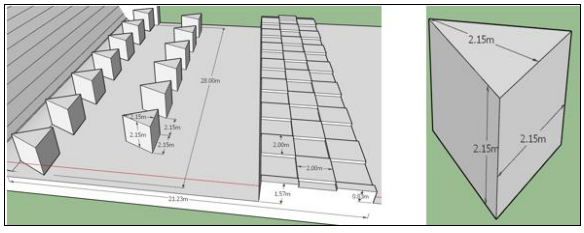

Fig 3.4. 6: Model M_5 with triangular basin blocks and chute blocks.

Model 6: Model with honeycomb basin blocks and chute blocks.
In Model 6, an approach was taken by replacing the conventional chute blocks and basin blocks with a honeycomb structure as of Model 2. All other dimensions were kept same.

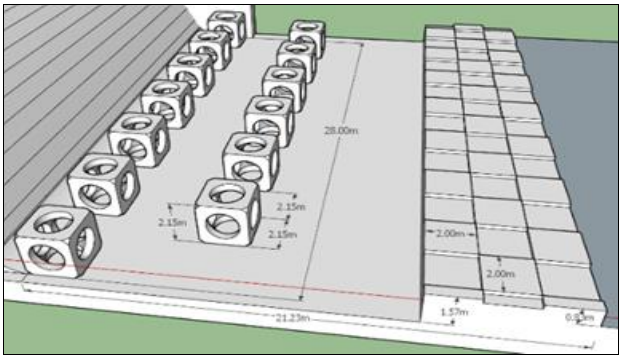

Model 7: Model with honeycomb basin blocks and chute blocks.
The blocks were introduced in two specific locations. Firstly, a series of honeycomb blocks were placed at 2.15 m D/S of the location of chute of the Model 1. Secondly, another series of honeycomb blocks were placed downstream (D/S) of the basin blocks, with a distance equal to the width of the blocks (i.e. 2.15 m) with a gap in alternate in-between. The arrangement can be seen as in the given diagram alongside.

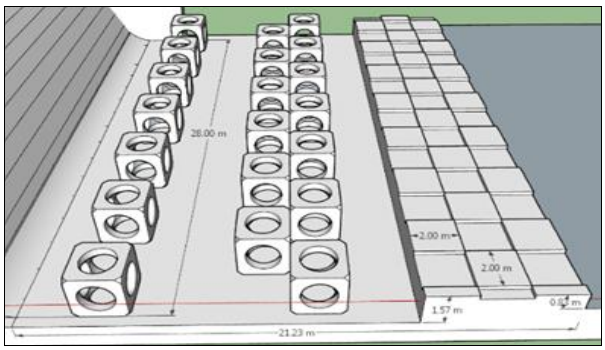

Model 8: Model with two series of honeycomb basin blocks and chute blocks.
In Model 8, chute blocks of Model 1 were removed so that there'd be enough space for the flow to pass through the baffle blocks attaining enough velocity. Similarly, the baffle blocks in Model 8 were shifted in at the D/S of the baffle blocks by the distance of twice the width of the blocks. This arrangement was intended to promote controlled energy dissipation and increase turbulence, potentially leading to improved energy dissipation.

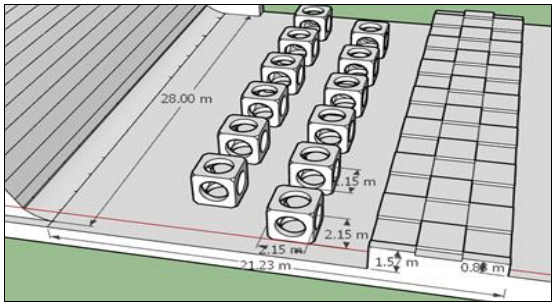

3.4 Model Optimization

The iterative process of improving the stilling basin's performance by changing its design components is explored in the model optimization phase. This section outlines the processes taken to examine various scenarios, modify basin appurtenances, and eventually end up at the most advantageous configuration that is consistent with predetermined study goals. Furthermore, Iterations of simulations were performed. For each iteration, the numerical model was modified, and simulations were conducted to simulate flow behavior, and energy dissipation.

3.5 Performance Evaluation

This part includes a thorough examination of simulation data, comparing the efficiency of various models in terms of energy dissipation, flow velocity, and flow depth. This portion have been carried out following parameters:

1. Depth Averaged Velocity for each Models at the particular point.
2. Flow Depth for each Models at the particular point.
3. Total Energy initially and after Energy dissipation.
4. Percentage of Energy dissipation.
5. Energy dissipation within limit on reducing the length of the stilling basin.

The tabular form for the first four points initially mentioned above, has been given below:

Table 3.5 1: Hydraulic parameters and % Energy Dissipation for length of the stilling basin, L= 21.5 m

For L=21.5 m	Model 1	Model 2	Model 3	Model 4	Model 5	Model 6	Model 7	Model 8
v_2 (m)	7.205	6.479	6.379	6.473	7.944	6.337	7.491	6.474
y_2 (m)	2.992	2.927	2.692	2.622	2.892	2.646	2.902	3.260
E_1 (m)	14.177	14.177	14.177	14.177	14.177	14.177	14.177	14.177
$E_{2,\ at\ x=35m}$ (m)	5.636	5.082	4.742	4.759	6.109	4.696	5.764	5.399
% Energy dissipation	60%	64%	67%	66%	57%	67%	59%	62%

Similarly, for each of the Models, a list of trials has been prepared that includes percentage reduction in length, length of the stilling basin for each model, and the number of trials. It has been tabulated as follows:

Table 3.5 2: List of Trials and corresponding % reduction in length

SN	Model number	Number of trials	% reduction at the last trial	Length at last trial(m)	Reason for rejection to proceed a new trial for comparison/Remarks
1	Model 1	1	0%	-	Base of comparison or Critical model
2	Model 2	5	12%	18.4m	Both T.E and velocity crossed the limit
3	Model 3	3	7.5%	19.6m	Both T.E and velocity crossed the limit
4	Model 4	2	5%	19.9m	T.E crossed the limit
5	Model 5	1	0%	0m	Both T.E and velocity crossed the limit
6	Model 6	2	5%	19.9m	T.E crossed the limit
7	Model 7	1	0%	-	Both T.E and velocity crossed the limit
8	Model 8	2	5%	19.9m	T.E for this Model = T.E. for Model 1

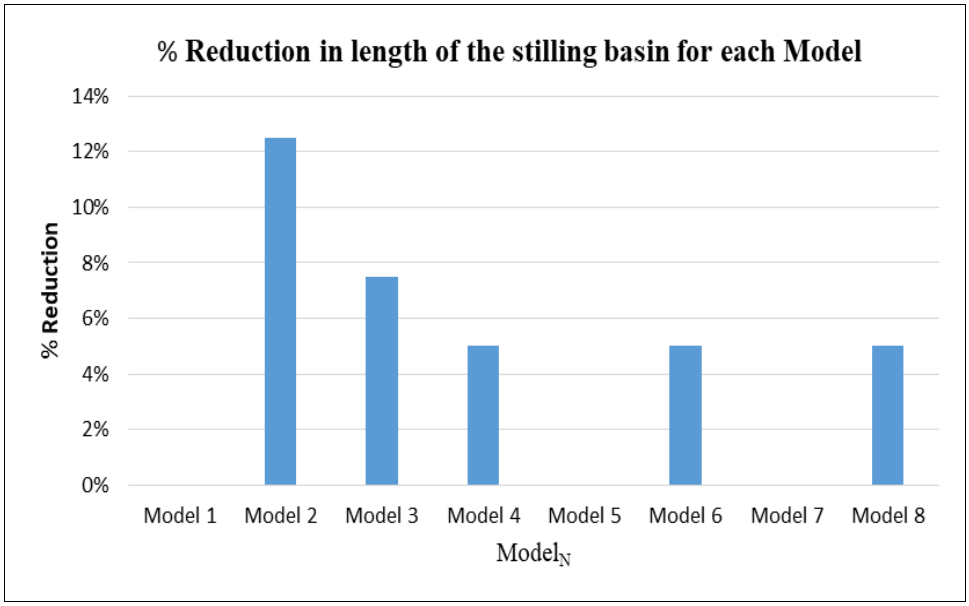

Fig: 3.5 1 A: Bar Chart representing % reduction in length for the maximum number of trials for each model

The hydraulic performance of the stilling basin for each model after the completion of the simulation for individual required number of trials has been compared for with the parameters including Total Energy, Depth Averaged Velocity and Flow Depth, downstream at x=35 m, measured from the heel of the dam.

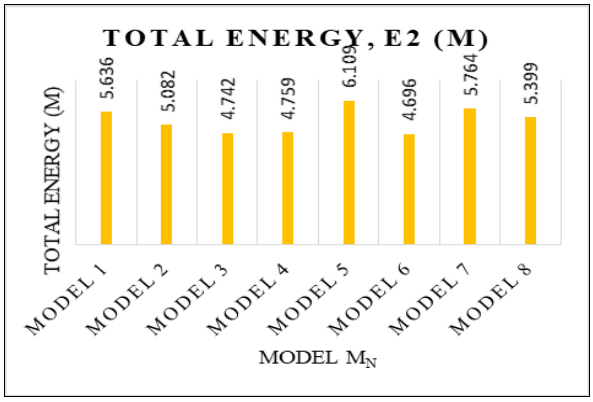

Fig: 3.5 2 Effect on Total Energy at x= 35 m

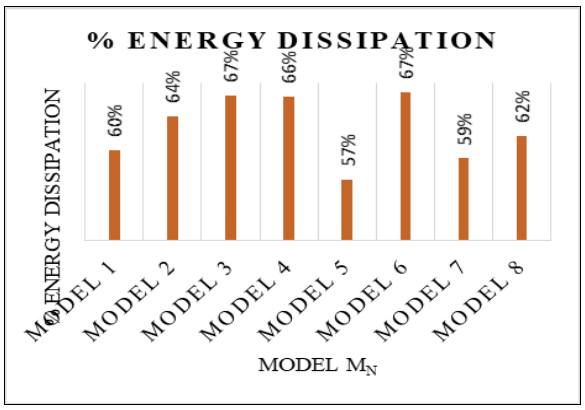

Fig: 3.5 3 Total Energy dissipation by each Model

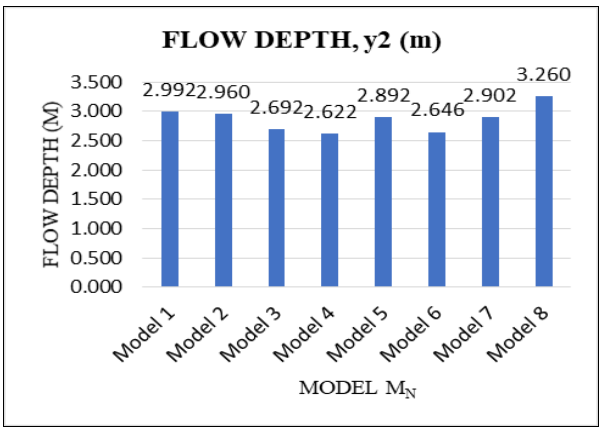

Fig: 3.5 4: Effect on the depth of the flow at x= 35 m

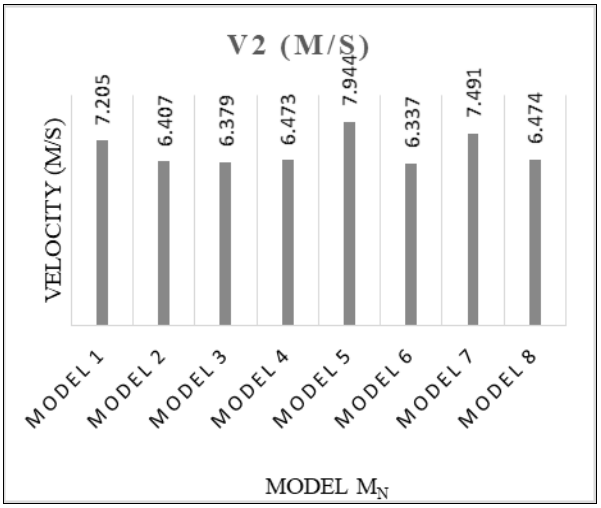

Fig: 3.5 5 Depth Averaged Velocity at x= 35 m for each model

Analyzing the hydraulic parameters from above bar charts, Model 3 and Model 6 perform best followed by Model 4 and Model 2 for Total Energy dissipation. Similarly, the flow velocity is least for model 6 followed by model 3. However, the model 5 and Model 8 crossed the limit for both Total Energy and flow velocity.

Results and discussion

The results demonstrate the spatial distribution of parameters such as total hydraulic head, providing a visualization of the energy dissipation process within the stilling basin. By observing the changes in total hydraulic energy at various locations, it becomes evident how the energy is dissipated as the flow progresses through the basin.

A number of trials were done with reduction in length of the stilling basin for each model until the threshold limit for the parameter is crossed. So, the trials required for each model varies accordingly, giving the optimized length of the stilling basin for each model. Altogether five trials were done for Model 2, which is maximum number of trials done among all the models. The tabulated form of trials for each Model have been given below:

Tables for Calibration of each Models

Table 4. 1: Trial 1: Initial case, Length of the stilling basin as per Model 1 (i.e. length of the stilling basin = 21.5 m)

SN	Model no.	Model 1	Model 2	Model 3	Model 4	Model 5	Model 6	Model 7	Model 8
1	Total energy at x= 35 m	5.636	5.082	4.742	4.759	6.109	4.696	5.764	5.399
2	Depth-averaged velocity at x= 35 m	7.205	6.479	6.379	6.473	7.944	6.337	7.491	6.474
3	Depth y_2 at x= 35 m	2.992	2.927	2.692	2.622	2.892	2.646	2.902	3.260

Table 4. 2: Trial 2, Length of the stilling basin reduced by 5% (i.e. length of the stilling basin = 20.42 m)

SN	Model no.	Model 1	Model 2	Model 3	Model 4	Model 6	Model 8
1	Total energy at x= 35 m	5.636	5.543	5.402	5.748	5.643	5.636
2	Depth-averaged velocity at x= 35 m	7.205	6.863	6.483	7.162	7.205	6.947
3	Depth y_2 at x= 35 m	2.992	3.140	3.257	3.131	3.022	3.175

Table 4. 3: Trial 3, Length of the stilling basin reduced by 7.5% (i.e. Length of the stilling basin = 19.88 m)

SN	Model no.	Model 1	Model 2	Model 3
	Total energy at x= 35 m	5.636	5.548	5.653

2	Depth-averaged velocity at x= 35 m	7.205	6.967	7.244
3	Depth y_2 at x= 35 m	2.992	3.073	2.978

Table 4. 4: Trial 4, Length of the stilling basin reduced by 10% (i.e. length of the stilling set = 19.35 m)

SN	Model no.	Model 1	Model 2
1	Total energy at x= 35 m	5.636	5.586
2	Depth-averaged velocity at x= 35 m	7.205	7.024
3	Depth y_2 at x= 35 m	2.992	3.069

Table 4. 5: Trial 5, Length of the stilling basin reduced by 12% (i.e. length of the stilling basin = 18.92 m)

SN	Model no.	Model 1	Model 2
1	Total energy at x= 35 m	5.636	5.647
2	Depth-averaged velocity at x= 35 m	7.205	7.233
3	Depth y_2 at x= 35 m	2.992	2.981

These results contribute to the understanding of energy dissipation in the stilling basin and can be used to optimize its design and enhance its overall efficiency. The results obtained after the simulation are further discussed below:

4.1 Total Energy, Depth Averaged Velocity and flow depth along the length of the stilling basin

The total hydraulic head E_2, is considered at 35 m from the origin, where the heel of the dam is considered as origin. The tabulated data and respecting graphs relating these parameters are shown below:

Table 4. 6: Change in Total Energy at 35 m with the change in length of the stilling basin for each model.

L (m)	% reduction	Total Energy at x = 35 m from the heel of the dam E2 (m)							
		Model 1	Model 2	Model 3	Model 4	Model 5	Model 6	Model 7	Model 8
	0.00%	5.636	5.082	4.742	4.759	6.109	4.696	5.764	5.399
20.42	5.00%	5.636	5.543	5.402	5.748	-	5.643	-	5.636
19.89	7.50%	5.636	5.548	5.653	-	-	-	-	-
19.35	10.00%	5.636	5.636	-	-	-	-	-	-
18.92	12.00%	5.636	5.636	-	-	-	-	-	-

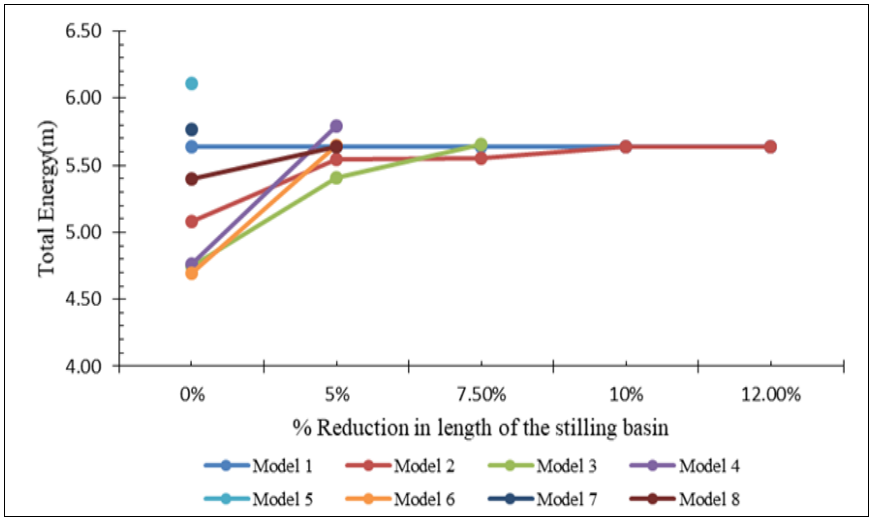

Fig 4. 3: Total Energy variation with % change in length of the stilling basin for each model.

Table 4. 7: Depth Averaged Velocity at 35 m with the change in length of the stilling basin.

L (m)	% reduction	Velocity at x = 35 m from the heel of the dam v2 (m)							
		Model 1	Model 2	Model 3	Model 4	Model 5	Model 6	Model 7	Model 8
	0.00%	7.205	6.479	6.379	6.473	7.944	6.337	7.491	6.474
20.42	5.00%	7.205	6.863	6.483	7.162	-	7.205	-	6.947
19.89	7.50%	7.205	6.967	7.244	-	-	-	-	-
19.35	10.00%	7.205	7.024	-	-	-	-	-	-
18.92	12.00%	7.205	7.233	-	-	-	-	-	-

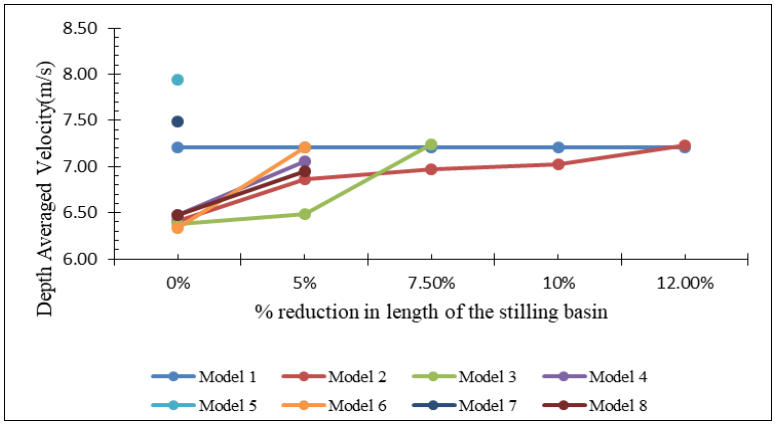

Fig 4. 4: Change in Depth Averaged Velocity with the change in length of the stilling basin.

Table 4. 8: Change in depth of the flow with the change in length of the stilling basin.

L (m)	% reduction	Depth at x = 35 m from the heel of the dam y_2 (m)							
		Model 1	Model 2	Model 3	Model 4	Model 5	Model 6	Model 7	Model 8
	0.00%	2.992	2.927	2.692	2.622	2.892	2.646	2.902	3.260
20.42	5.00%	2.992	3.140	3.257	3.131	-	3.022	-	3.175
19.89	7.50%	2.992	3.073	2.978	-	-	-	-	-
19.35	10.00%	2.992	2.992	-	-	-	-	-	-
18.92	12.00%	2.992	2.992	-	-	-	-	-	-

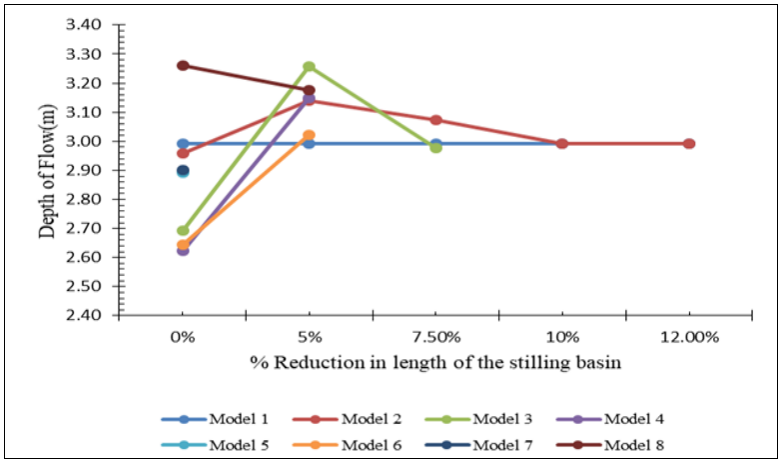

Fig 4. 5: Change in Depth of the Flow with the change in length of the stilling basin.

4.2 Discussion Relating Comparison of Initial and Final Trials for Each Models

4.2.1 Model 1

Using the hydraulic parameters at steady state condition of the flow including Hydraulic depth, Free surface elevation, Depth averaged velocity and Total hydraulic head, the graph was plotted along the flow direction as in figure 4.6 below:

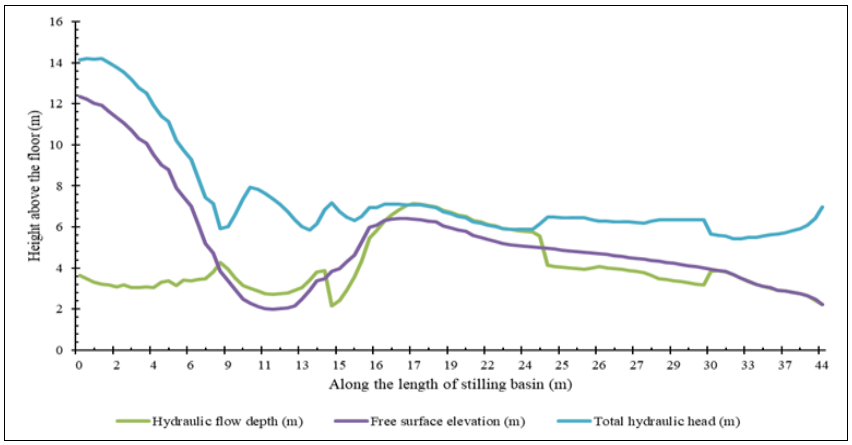

Fig: TE, Hyfd and Hyel in X-Z plane for Model 1 at steady state condition.

The total energy, E_1, at the beginning has a value of 14.177 m. As we move downstream, at 35 m from the heel of the dam where the actual river bed starts, the total hydraulic head decreases to 5.636 m. This reduction in total energy highlights the effectiveness of the stilling basin in dissipating energy and reducing the flow's destructive potential. The 2D and 3D figure that depicts the total hydraulic head obtained from the simulation has been represented by different colors at every location of the section and is shown in the figures below.

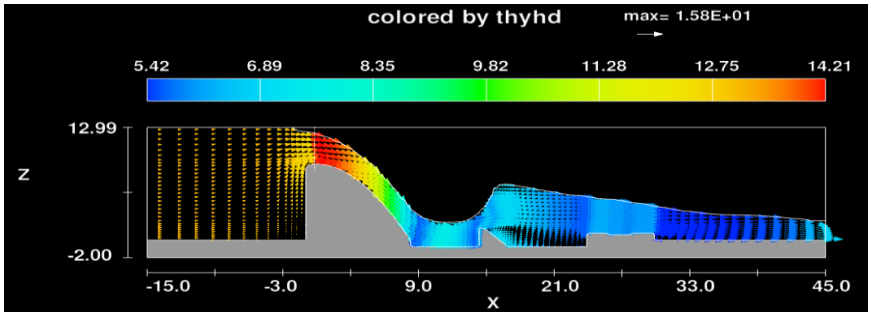

Fig: Total hydraulic head in X-Z plane for Model 1 at steady state condition.

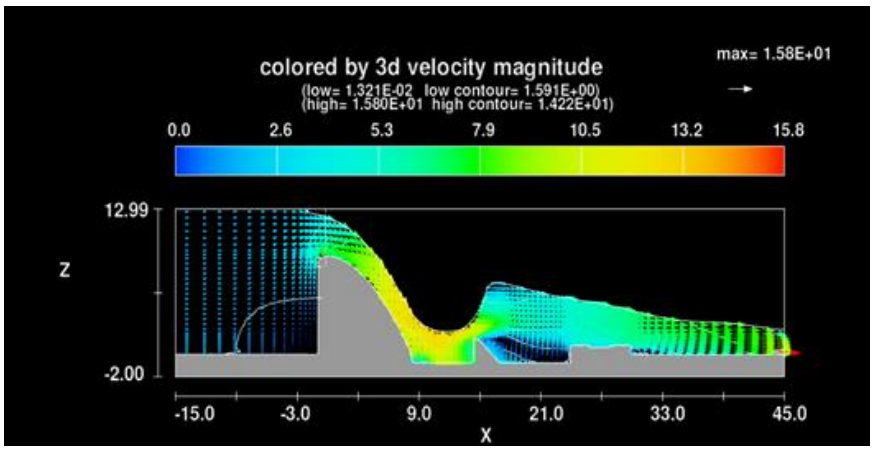

Fig: Depth Averaged Velocity in X-Z plane for Model 1 at steady state condition.

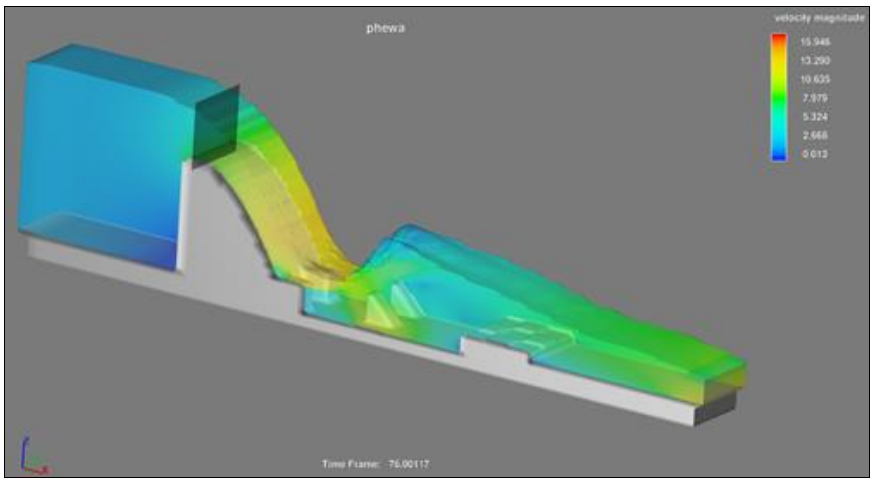

Fig: Depth Averaged Velocity in 3D view for Model 1 at steady state condition.

4.2.2 Model 2

After extraction of the hydraulic data at steady condition, from the simulation of Model 2, it was compared with Model 1 in terms of Total Energy and Depth averaged velocity, and found to be less than that of Model 1. Hence, the stilling basin of this type is capable of dissipating energy with smaller length of the stilling basin. The hydraulic parameters obtained after running the initial state as per the study with standardized size have been plotted in the graph as shown in figure.

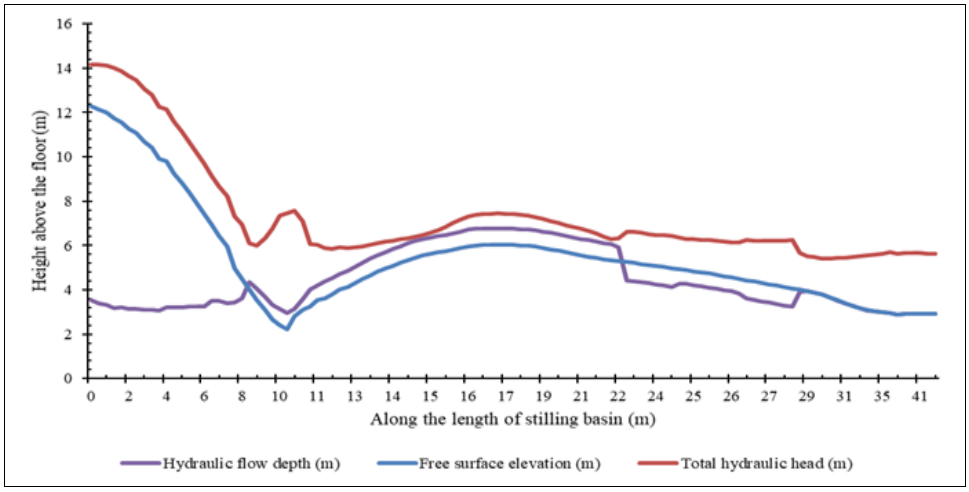

Fig: TE, Hyfd and Hyel in X-Z plane for Model 2 at steady state condition.

So, this model was further modified by reducing the length of the stilling basin by 5% of the initial length, hence, new length = 20.4 m and, the simulation was run keeping other parameters unchanged.

Overall, five trials were done, with the length of the stilling basin, 12% less than the initial length of the stilling basin, the length of 18.92 m. For this case, the total energy at 35 m was found to be 5.647 m and depth averaged velocity was found to be 7.233 m/s. So, both the Total Energy and Depth Averaged Velocity crossed the threshold for our comparison. Hence, the length of the stilling basin couldn't be reduced further. The point where the limit was compared was determined using the graph plotted for depth averaged velocity and found to be at 11.8% of the initial length of the stilling basin. So, the final length of the stilling basin using this model becomes 18.9 m.

Here, due to the shape of the honeycomb structures, the energy dissipation occurred due to the shape of the blocks allowing the flow through the voids within the blocks rather than the impact.

4.2.3 Model 3

For Model 3, for the length of the stilling basin on running simulations and analyzing, was found to be 7.2% less than original length (i.e. revised length = 19.95 m) with the total energy equal to that of critical/threshold limit at 35 m D/S of the heel of the dam as the threshold Depth Averaged Velocity is obtained earlier than the Total Energy.

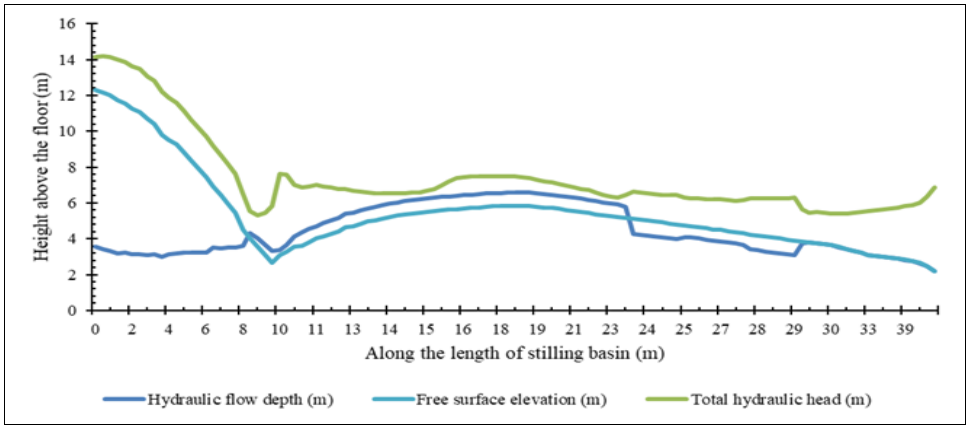

Fig: TE, Hyfd and Hyel in X-Z plane for Model 3 at steady state condition.

4.2.4 Model 4

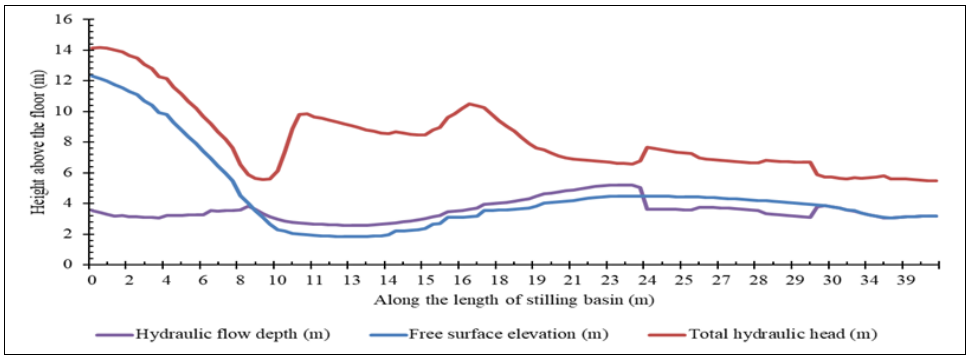

Fig: TE, Hyfd and Hyel in X-Z plane for Model 4 at steady state condition.

For Model 4, the length of the stilling basin, on running simulations and by analysis, it was found to be 4.5% less (i.e. 20.53m) than original length, with the total energy as of Model1 (i.e. 5.636 m) at 35 m D/S of the heel of the dam and the threshold Depth Averaged Velocity is already less than that of Model 1 with the magnitude of 7.205 m/s.

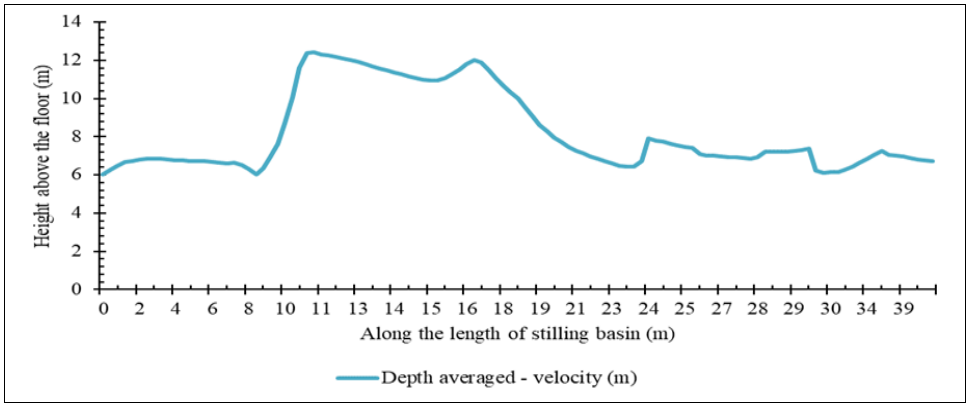

Fig: Davel in X-Z plane for Model 4 at steady state condition.

4.2.5 Model 5

After the extraction of the hydraulic data from the simulation of Model 5, it was compared with Model 1 both in terms of Total Energy and Depth averaged velocity, and found to be more than that of Model 1. So, this model was not further modified as the hydraulic limits considered for this study has been crossed at first trial with the same length as of Model 1.

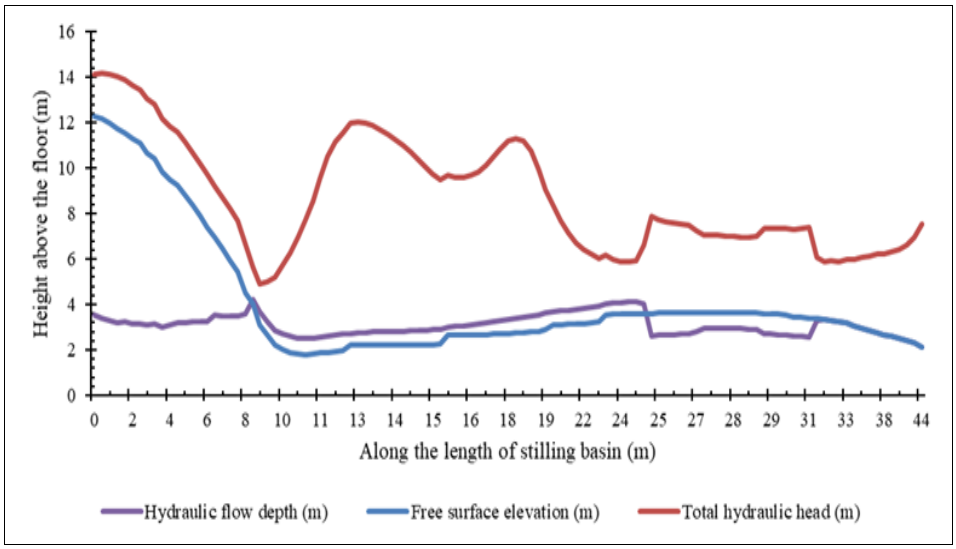

Fig: TE, Hyfd and Hyel in X-Z plane for Model 5 at steady state condition.

The main concept for this Model initially was increasing the length of the flow within the basin using the triangular blocks. However, the model didn't perform well, hence, rejected at the first trial.

4.2.6 Model 6

After the extraction of the hydraulic data from first trial of Model 6, on comparing with Model 1 both in terms of Total Energy and Depth averaged velocity, and found to be less than that of Model 1. So, this model was further modified by reducing the length by 5% of the initial length, so that, the length becomes 20.42 m, and, the results and the same parameters as earlier were compared that crossed the critical value for Total Energy. However, the Depth Averaged Velocity didn't cross the threshold that was considered critical for our model.

Hence, on interpolation of the Total Energy vs. reduction in length, the Total Energy crossed the limit at 4.9% reduction in length. That gives the length of the stilling basin for this configuration to be 20.44 m.

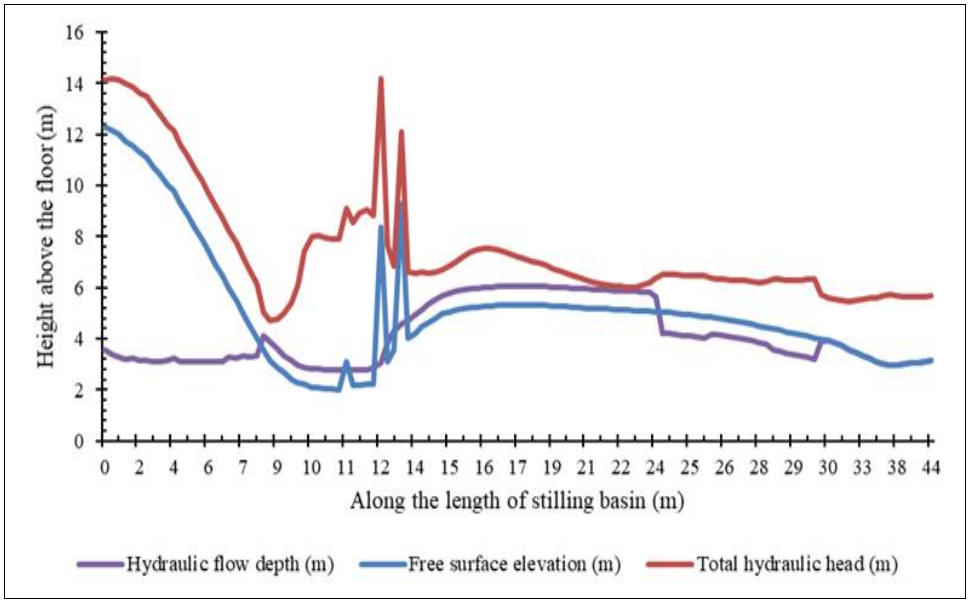

Fig 4. 20. 1: TE, Hyfd and Hyel in X-Z plane for Model 6 at steady state condition.

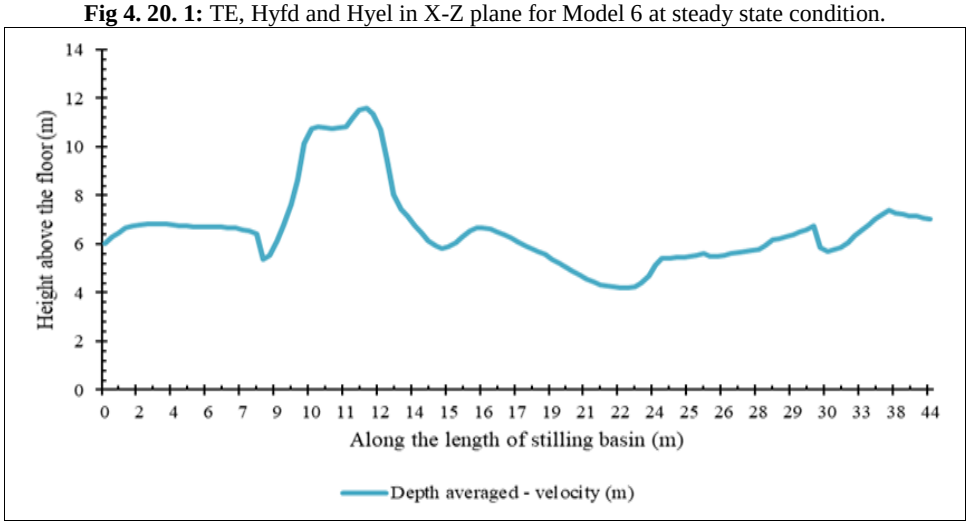

Fig 4. 21. 2: Davel in X-Z plane for Model 6 at steady state condition.

4.2.7 Model 7

After the extraction of the hydraulic data from the simulation of Model 7, it was compared with Model 1 both in terms of Total Energy and Depth averaged velocity, and found that the Total Energy to be less than that of Model1, while the Depth Averaged velocity was more than that of Model1. That means, the stilling basin of this type could not be modified further.

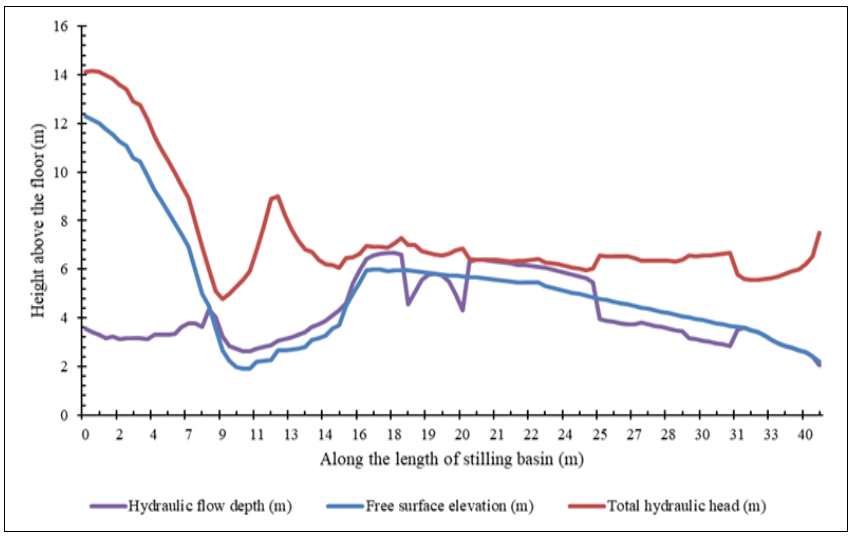

Fig: TE, Hyfd and Hyel in X-Z plane for Model 7 at steady state condition.

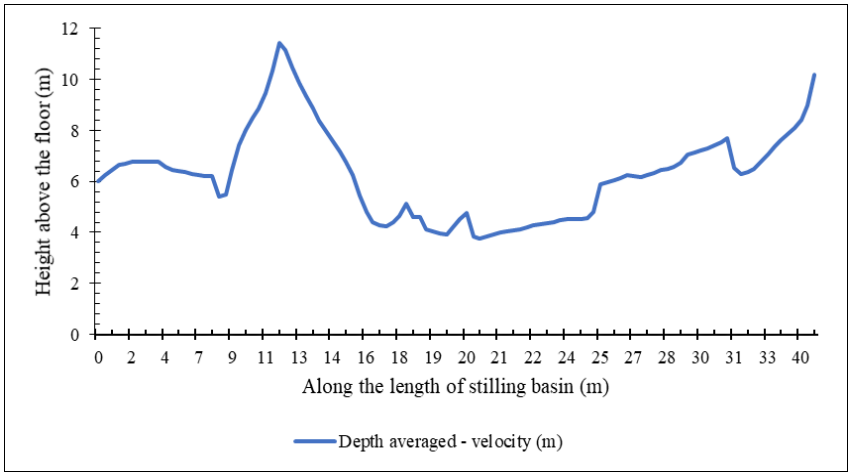

Fig: Davel in X-Z plane for Model 7 at steady state condition.

4.2.8 Model 8

The hydraulic data from the simulation of Model 8 was extracted and then it was compared with Model 1 both in terms of Total Energy and Depth averaged velocity, and found to be less than that of Model 1. On reducing 5% from the initial length, and after running the simulation it was found to be 4.9% less (i.e. 21.5m - 2.45 m = 1.05 m) than original length. So, the optimized length of the stilling basin becomes 20.45 m. The representative figures relating this model for Total Energy and Depth Averaged Velocity at optimum length of the stilling basin are given below:

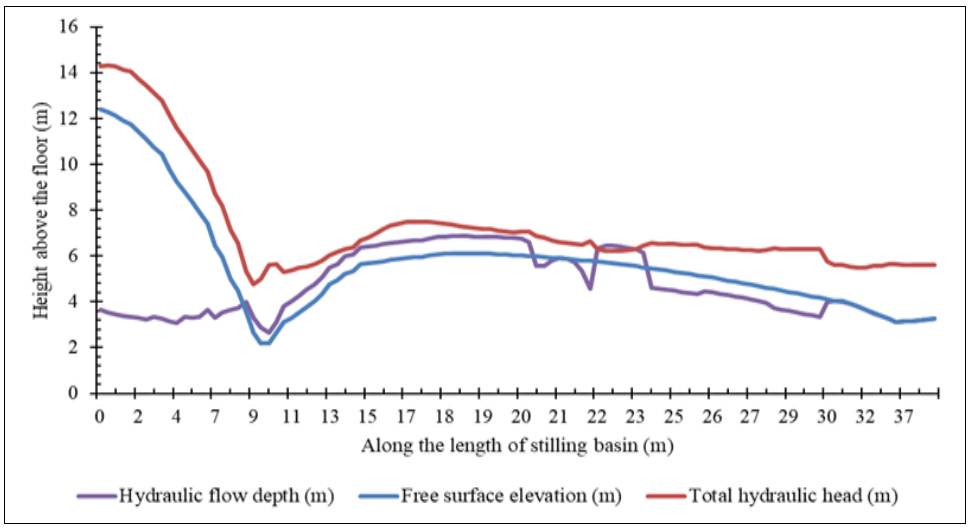

Fig 4. 1. 1: TE, Hyfd and Hyel in X-Z plane for Model 8 at steady state condition.

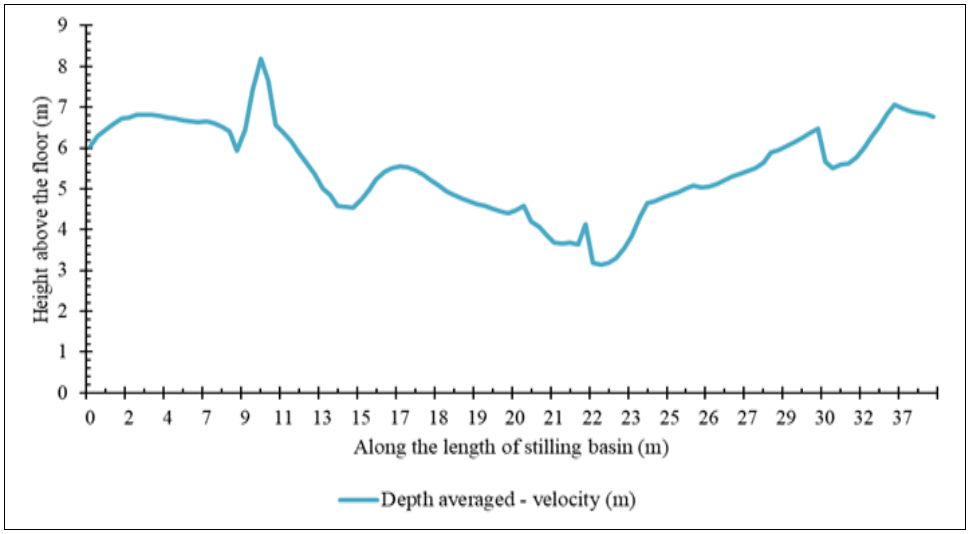

Fig 4. 26. 2: Davel in X-Z plane for Model 8 at steady state condition.

Conclusion

Among the study of eight different models and comparing each of them with Model1 in terms of Total Energy, Depth Averaged Velocity and Depth of flow, six of the models performed best in terms of all the hydraulic parameters. After further analysis of each model by changing the dimension of the stilling basin, Model 2 performed best even after the reduction in length of the stilling basin by 11.8%. It shall be noted that the Model 2 is composed of honeycomb structure as baffle blocks.

Similarly, Model 3 performed best after Model 2 with 7.5% reduction in length of the stilling basin, however, the velocity limit for this model crossed the limit with total energy less than the threshold limit. Also, Model 4, Model 6 and Model 8 with 5% reduction in length of the stilling basin. For this model, total energy crossed the threshold limit for our study, while the velocity remained less than the threshold limit.

Conversely, Model 5 and Model 7 were not changed in length as the hydraulic parameters exceeded the threshold of the study. Both the Model 5 and Model7 exceeded the total energy and depth averaged velocity with energy dissipation of 57% and 59% respectively, least among all the models studied. Similarly, the Model 7 also exceeded the threshold limit for the hydraulic parameters (including Total Energy and Depth Averaged Velocity) of the study by small amount.

So, Model 2, a model with honeycomb structure as baffle blocks performed the best among all the models that were studied, with the energy dissipation of 60% even after the reduction of the length of the stilling basin by 11.8% of the length of Model 1 as prescribed by USBR.

Hence, a viable approach to maximizing energy dissipation and obtaining the requisite hydraulic performance is to incorporate honeycomb structures as baffle blocks within the stilling basin. Because of their detailed shape, honeycomb structures are particularly useful for efficiently reducing the energy of incoming flows. This is ascribed to the honeycomb pattern's distinctive geometrical layout, which produces a maze-like network of interconnected voids and obstacles that promote increased turbulence and energy dispersion.

The thorough investigation done through numerical modeling and simulation has shown how honeycomb structures affect energy dissipation in the stilling basin favorably. As the flow passed through the honeycomb structures, the simulation results consistently showed considerable reductions in flow energy levels. This result can be due to the intricate flow interactions that take place within the honeycomb's interstitial spaces. These interactions encourage quick energy loss through frictional losses, eddies, and vortices.

A further benefit of using honeycomb structures is that the stilling basin's size can be optimized. The complex honeycomb shape allows for effective energy dissipation across a smaller area, hence lowering the length of the basin while retaining high levels of energy reduction. In situations where limited space is available, this optimization potential is essential.

In conclusion, a fresh and successful method for enhancing stilling basin performance is introduced by integrating honeycomb structures as baffle blocks. The observed increases in energy dissipation and the subsequent possibility for size optimization indicate the viability of implementing this creative design approach. Future research into honeycomb structures for improving the hydraulic effectiveness of stilling basins is warranted in light of these findings, which provide insightful information for hydraulic engineering techniques.

References

1. Hayder AM. A study on stilling basin with semi-circular rough bed. Jordan Journal of Civil Engineering. 2017;11(2).
2. Hix KD. Experimental evaluation of a honeycomb structure in open channel flows [dissertation]. Rolla: Missouri University of Science and Technology; 2020.
3. Tabatabai MHABM. Numerical study of flow patterns in stilling basin with sinusoidal bed using Flow. AENSI Journals. 2014.
4. Babaali HS, Hamidreza A. Computational modeling of the hydraulic jump in the stilling basin. Arabian Journal for Science and Engineering. 2014.
5. Abbas HAAM. Effect of baffle block configurations on characteristics of hydraulic jump in adverse stilling basins. MATEC Web of Conferences. 2018;162:03005.
6. Bestawy A. New shapes of baffle piers used in stilling basins as energy dissipators. Asian Transactions on Engineering (ATE). 2013;3(1).
7. Zaffar M, Hussain IH. Hydraulic investigation of stilling basins of the barrage before and after remodelling using FLOW-3D. Water Supply. 2023 Feb.
8. Lopez-Jimenez PA, Boulanger A. Numerical analysis of hydraulic jumps using OpenFOAM. Journal of Hydroinformatics. 2015.
9. Javed SMSN, Farhoudi SHA. Pressure fluctuation around chute blocks of SAF stilling basin. Journal of Agricultural Science and Technology. 2010 Mar.
10. De Padova D, Mossa M. Hydraulic jump: A brief history and research challenges. Water. 2021;13(1733). https://doi.org/10.3390/w13121733
11. Garcia-Bartual R, Del Valero JM. Optimisation of stilling basin chute blocks using a calibrated multiphase RANS model. In: 5th International Junior Researcher and Engineer Workshop on Hydraulic Structures; 2014 Aug.
12. Falvey HT. Cavitation in chutes and spillways. Denver: USBR Engineering Monograph; 1990.
13. Hirt CW, Nichols BD. Volume of fluid (VOF) method for the dynamics of free boundaries. Journal of Computational Physics. 1981;39(1):201-225.
14. Kramer KH, Hager WH, Minor HE. Development of air concentration on chute spillways. Journal of Hydraulic Engineering. 2006;132(9):981-993.
15. Basco JR, Adams DR. Drag force on baffle block in hydraulic jumps. Journal of the Hydraulics Division, ASCE. 1971;97(10):1653-1666.
16. Blaisdell FW. The SAF stilling basin. Minneapolis: US Dept. of Agriculture, Soil Conservation Service, St. Anthony Falls Hydraulic Lab; 1943.
17. Farhoudi J, Narayanan R. Force on slab beneath hydraulic jump. Journal of the Hydraulics Division, ASCE. 1991;117(6):843-856.
18. Peterka AJ. Hydraulic design of spillways and energy dissipators. Denver: A Water Resources Technical Publication, Engineering Monograph; 1984.

19. Pfister M, Hager WH. Deflector-jets affected by pre-aerated approach flow. Journal of Hydraulic Research. 2012;50(5):498-506.
20. Bollaert EFR, Schleiss AJ. Scour of rock due to the impact of plunging high velocity jets: A state-of-the-art review. Journal of Hydraulic Research. 2003;41(5):451-464.
21. Garg SK. Irrigation and Hydraulic Structures. New Delhi: Khanna Publishers; 2006.
22. Novak P, Moffat AI, Nalluri C, Narayanan R. Hydraulic Structures. 4th ed. London: Taylor & Francis; 2007.

Annex

FAVO Ring each models and the initial condition of fluid

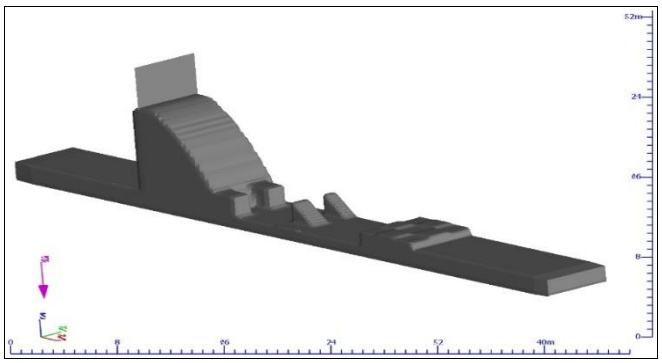

M1: View of setting Initial Condition

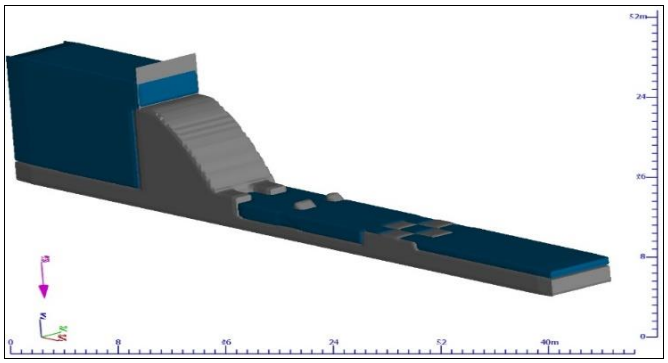

M1: View after FAVORing

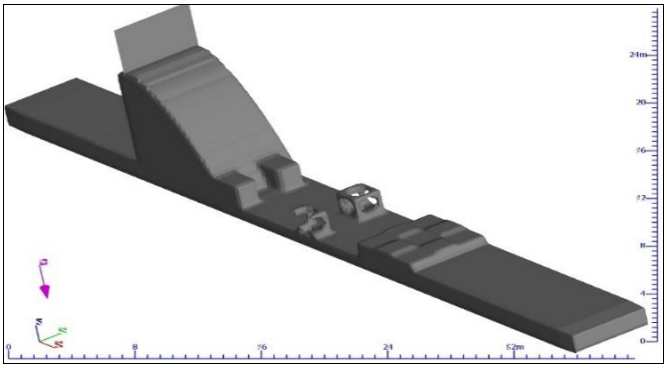

M2: View after FAVORing

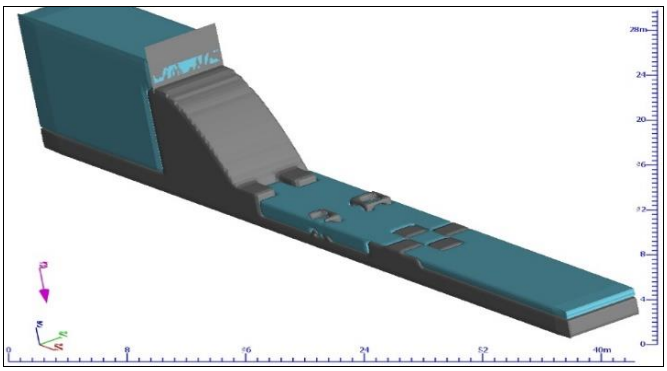

M2: View of setting Initial Condition

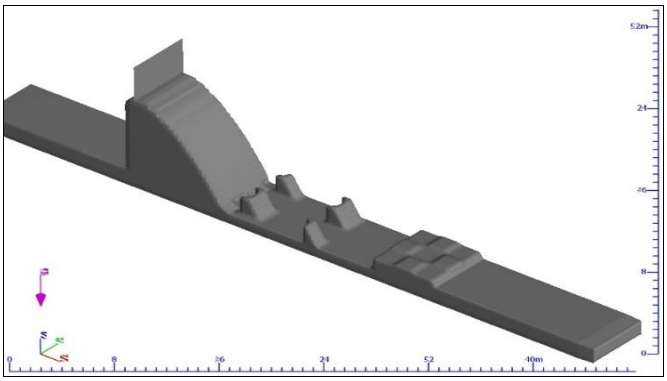

M3: View after FAVORing

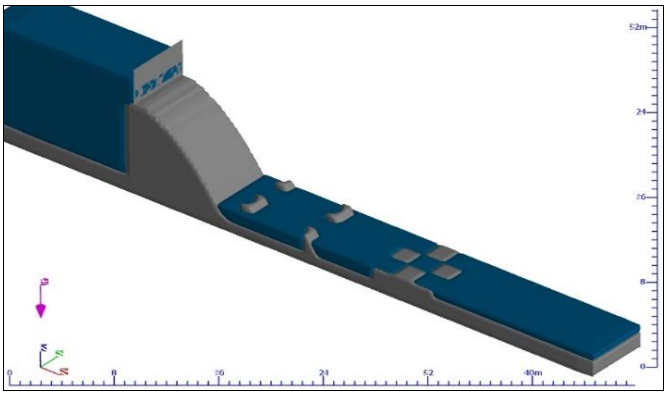

M3: View of setting Initial Condition

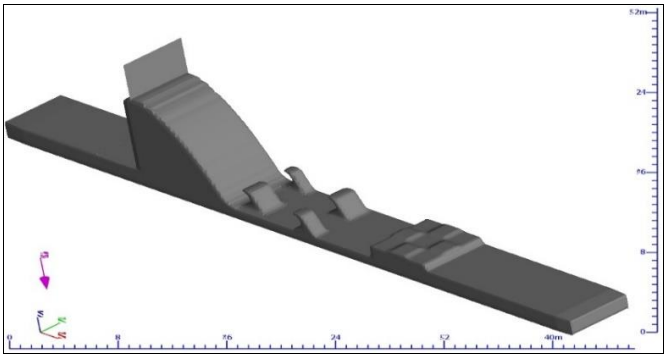

M4: View after FAVORing

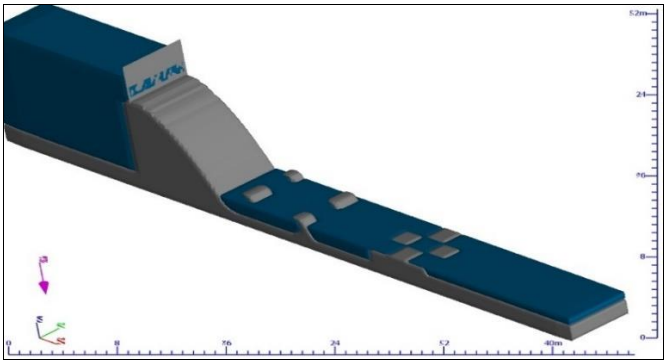

M4: View of setting Initial Condition

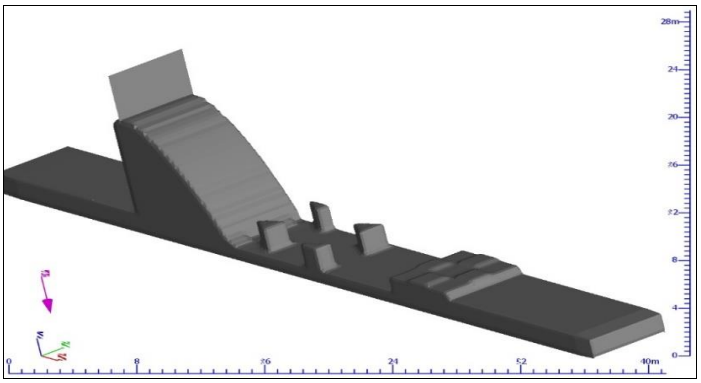

M5: View after FAVORing

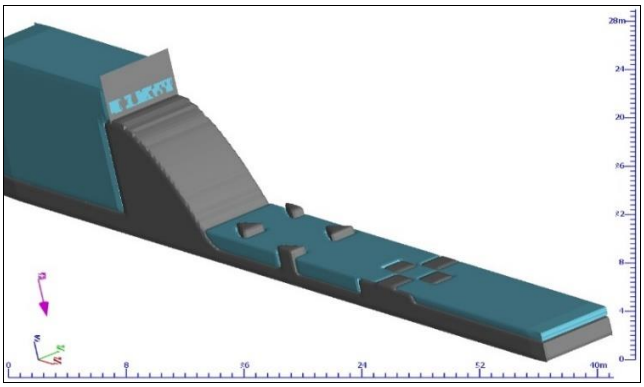

M5: View of setting Initial Condition

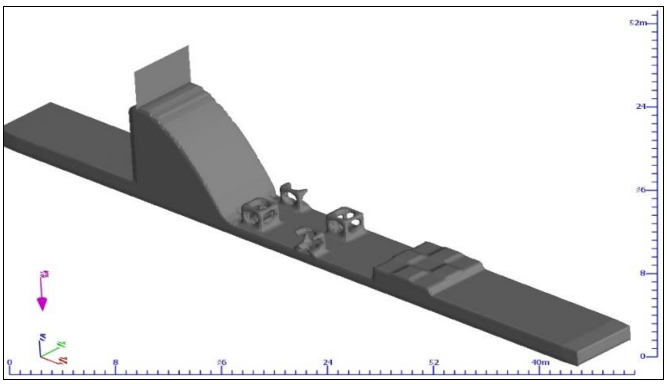

M6: View after FAVORing

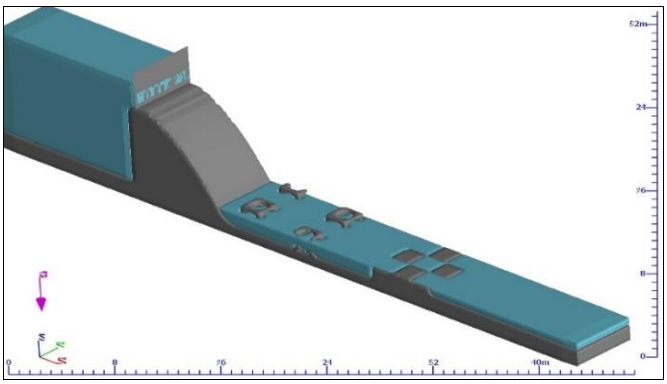

M6: View of setting Initial Condition

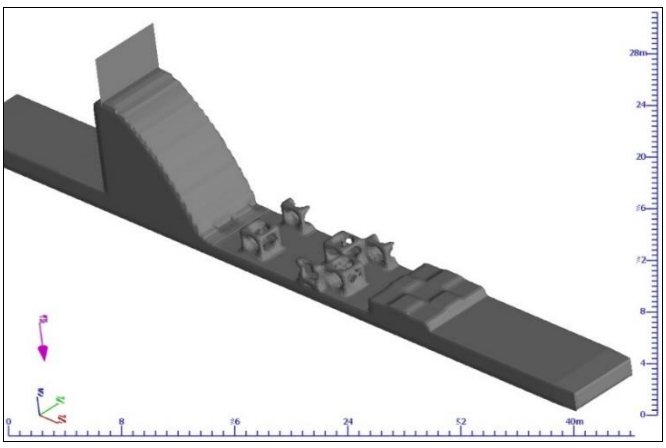

M7: View after FAVORing

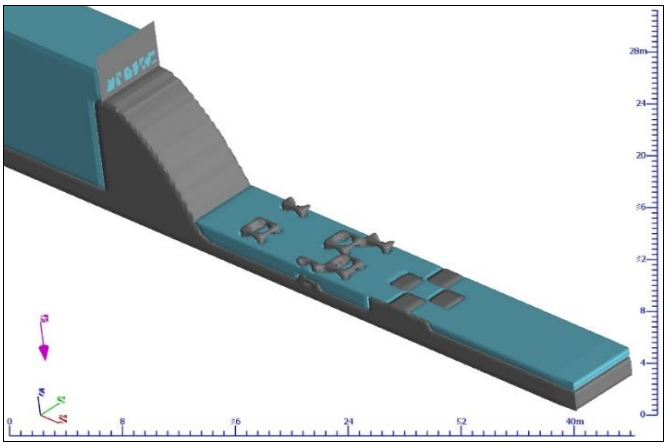

M7: View of setting Initial Condition

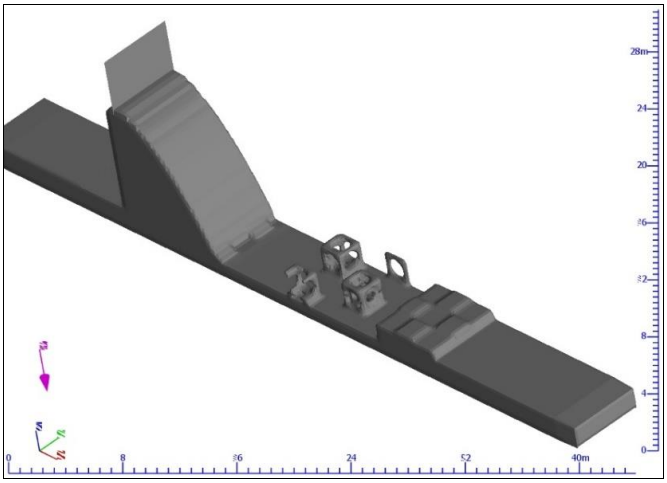

M8: View after FAVORing

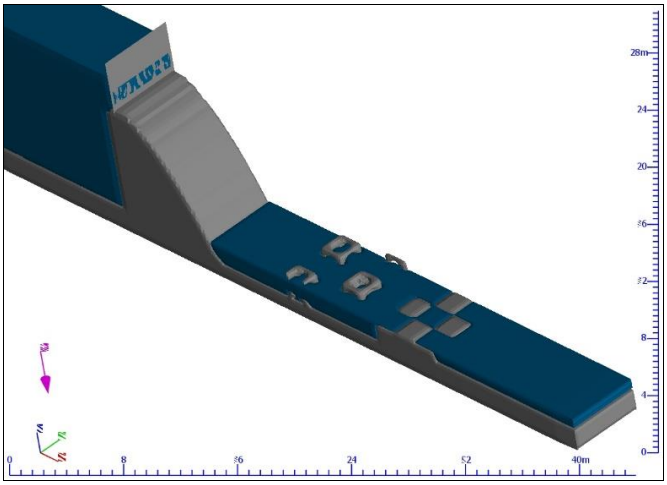

M8: View of setting Initial Condition

3D pictures of each models at steady state condition

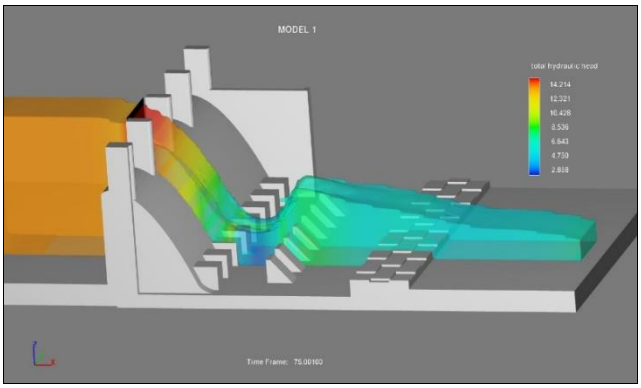

M1: Total hydraulic head

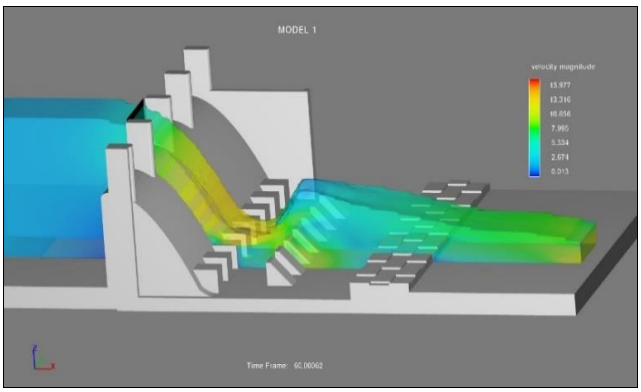

M1: Velocity magnitude

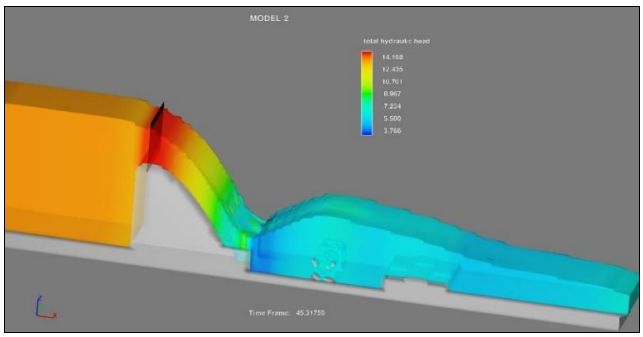

M2: Total hydraulic head

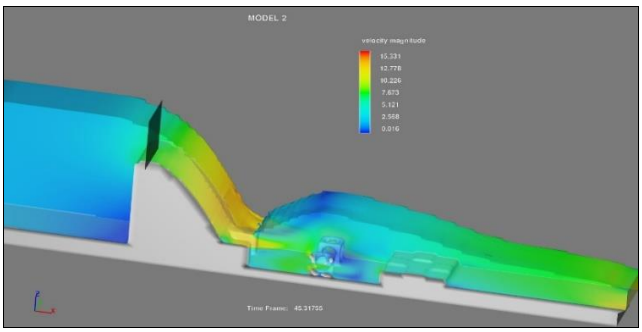

M2: Velocity magnitude

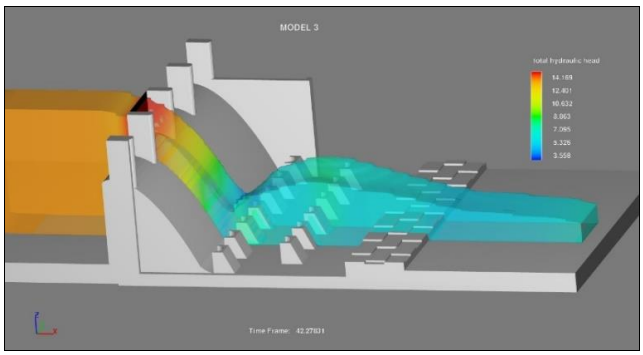

M3: Total hydraulic head

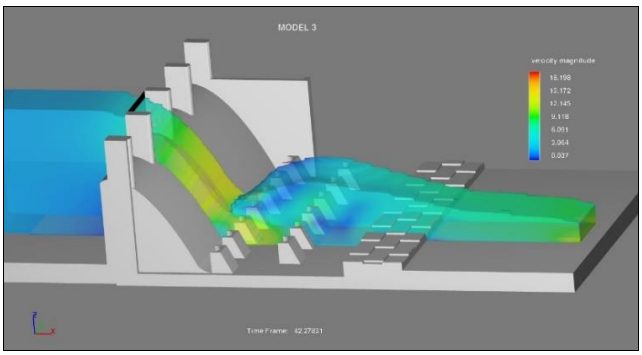

M3: Velocity magnitude

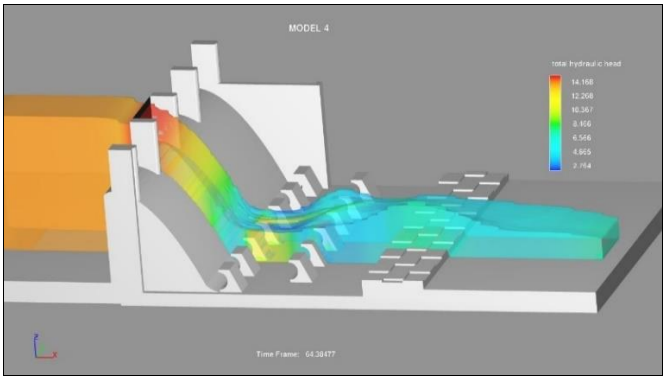

M4: Total hydraulic head

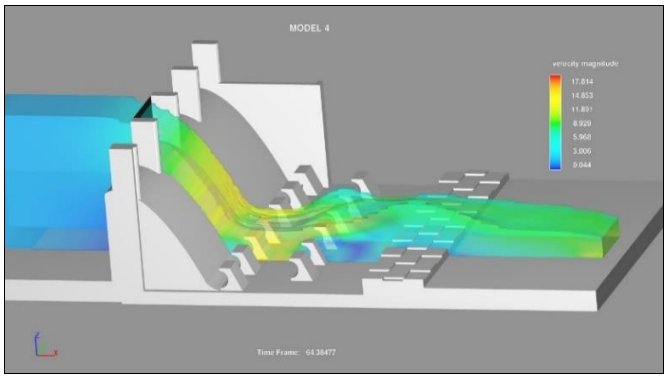

M4: Velocity magnitude

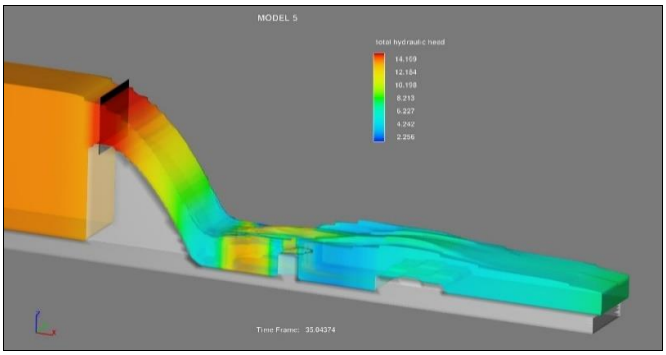

M5: Total hydraulic head

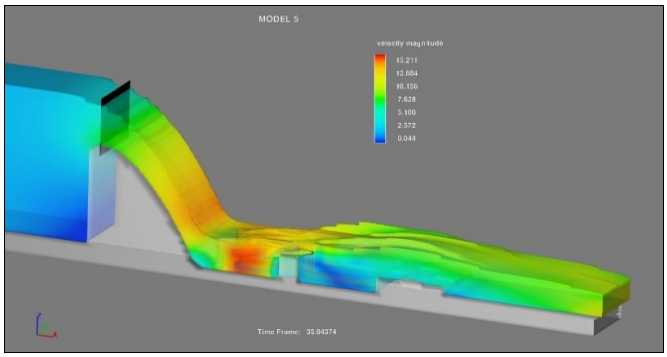

M5: Velocity magnitude

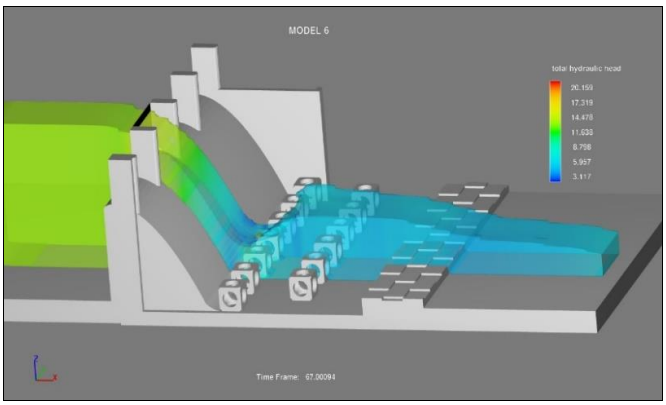

M6: Total hydraulic head

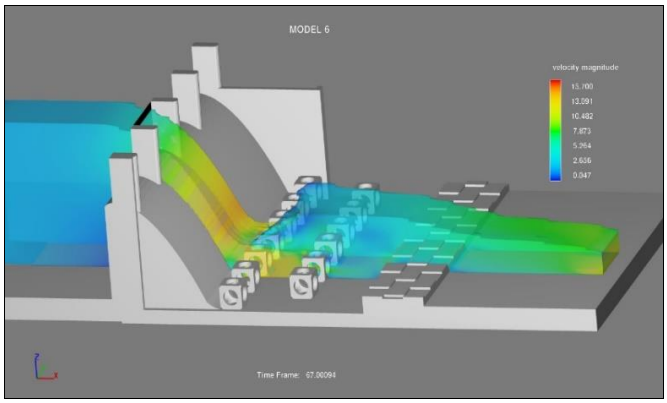

M6: Velocity magnitude

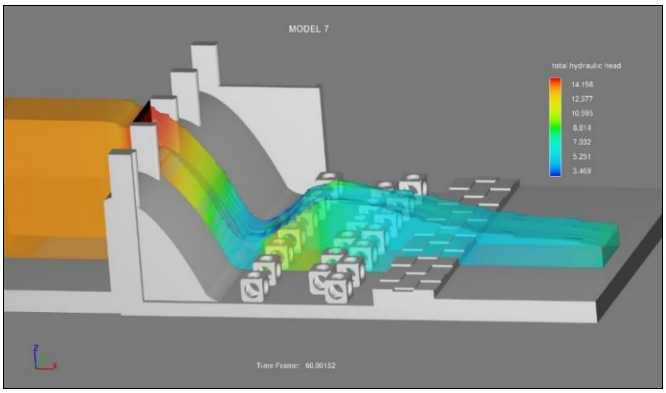

M7: Total hydraulic head

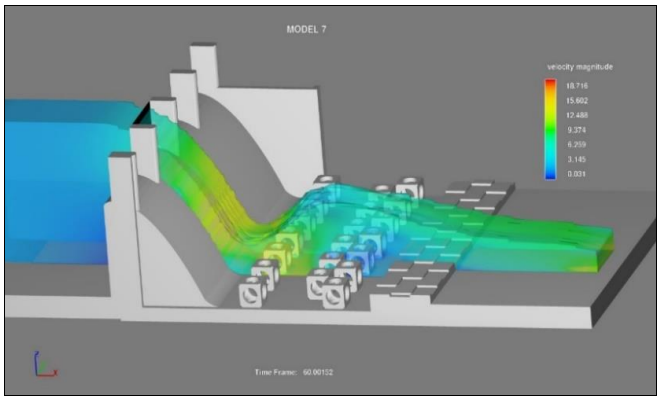

M7: Velocity magnitude

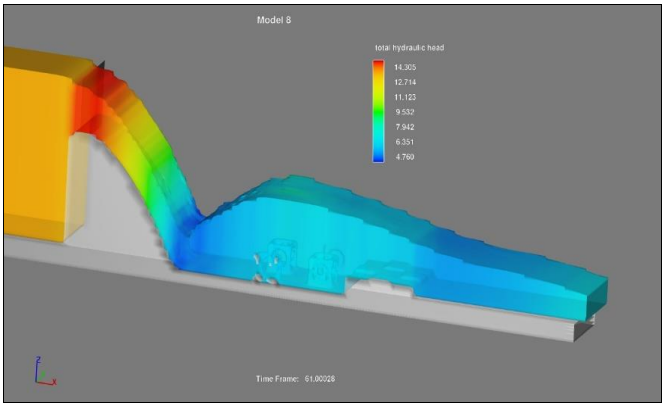

M8: Total hydraulic head

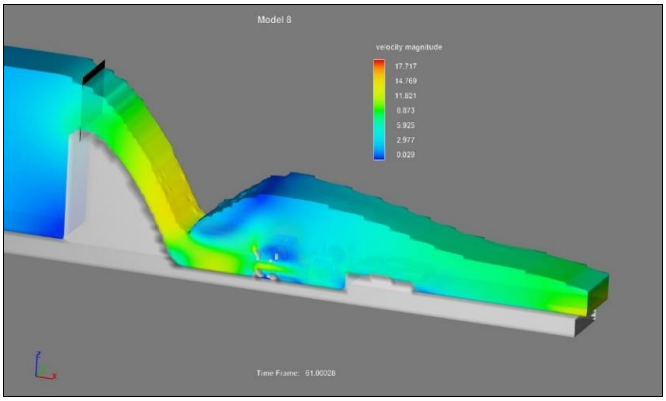

M8: Velocity magnitude

Sample 2D figures for total hydraulic head, velocity magnitude and depth averaged velocity obtained from simulation.

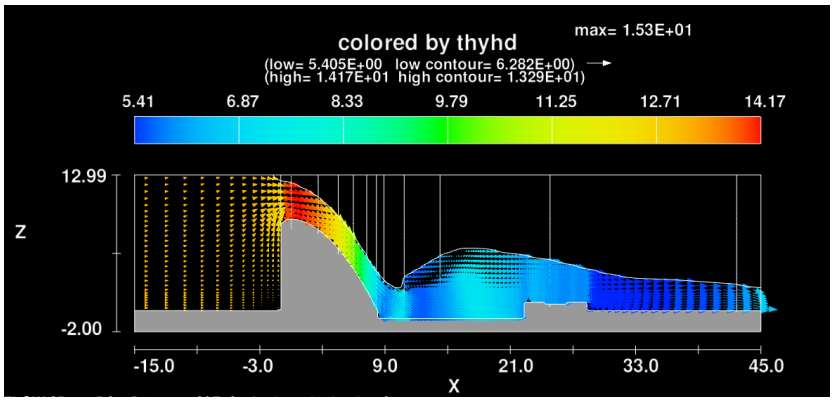

Fig: Total Hydraulic head for M2 with 12% reduction in length at steady state condition.

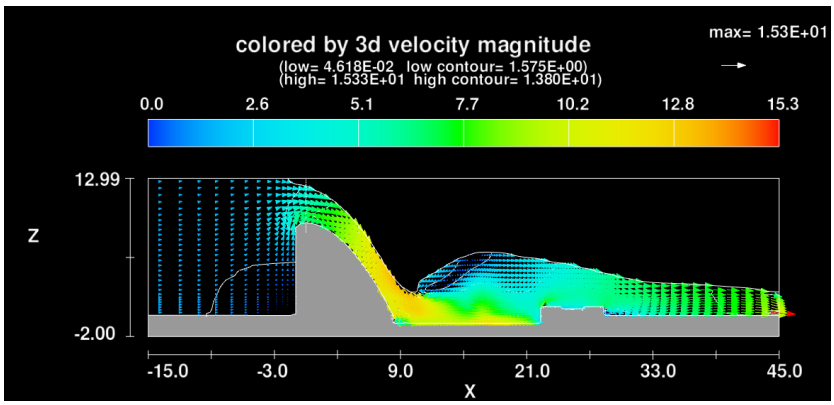

Fig: Velocity Magnitude for Model 2 with reduction of length by 12% at steady state

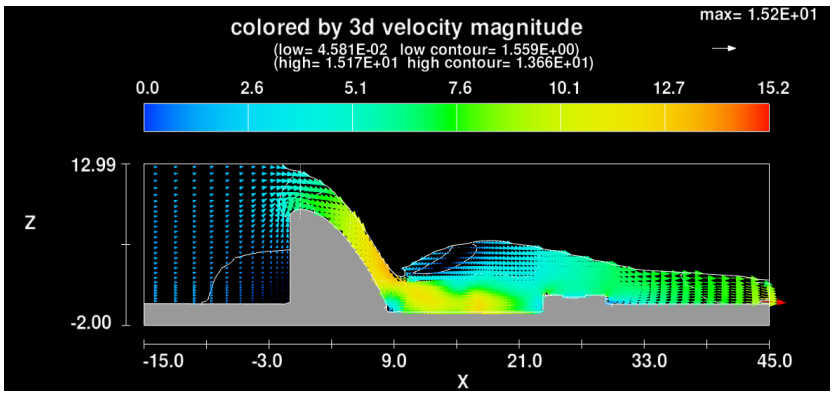

Fig: Model3 at steady state condition for 7.5% reduction in length

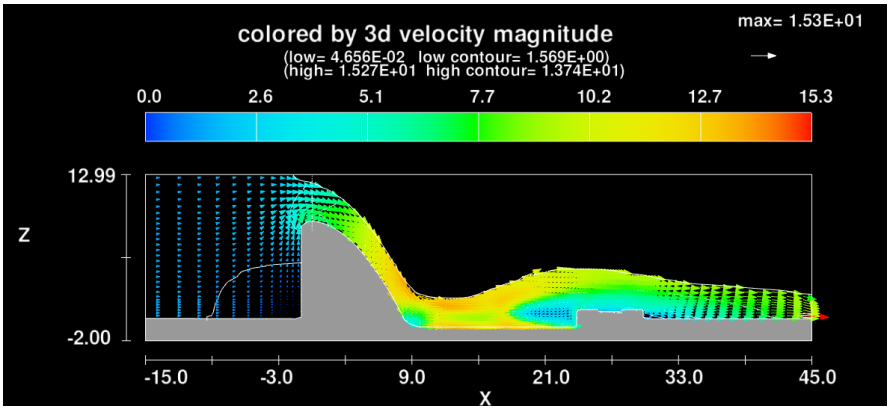

Fig: Model4 at steady state condition for 5% reduction in length

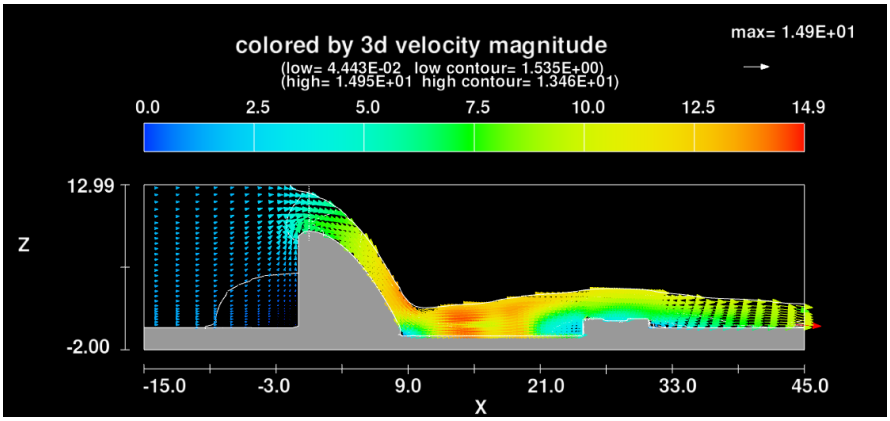

Fig: Davel for M5 at steady state

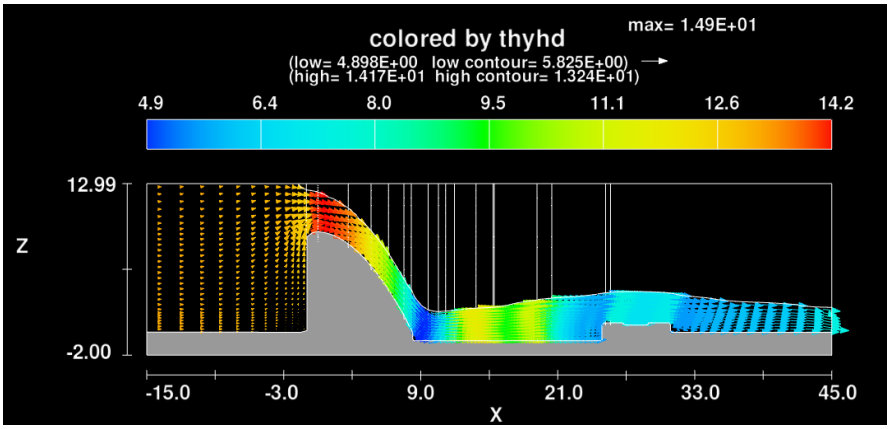

Fig: Thyhd for M5 at steady state

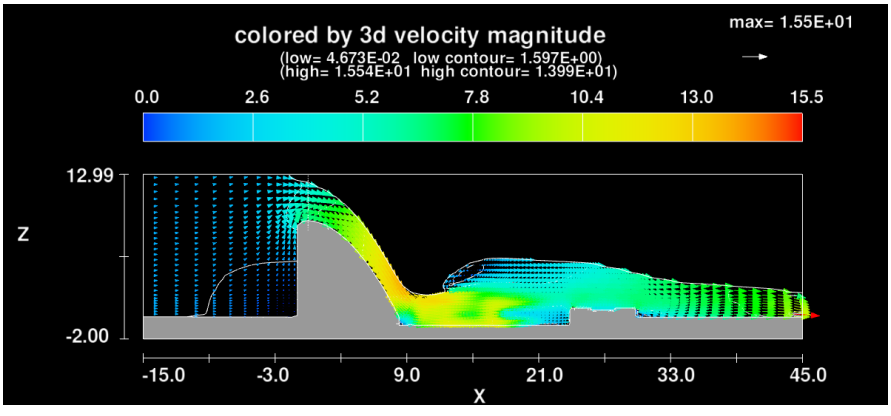

Fig: Davel for M6 with 5% reduction in length at steady state condition.

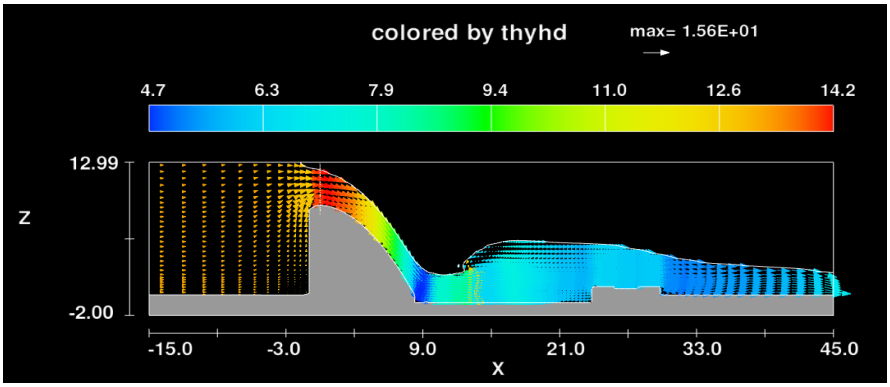

Fig: Thyhd for M6 with 5% reduction in length at steady state condition

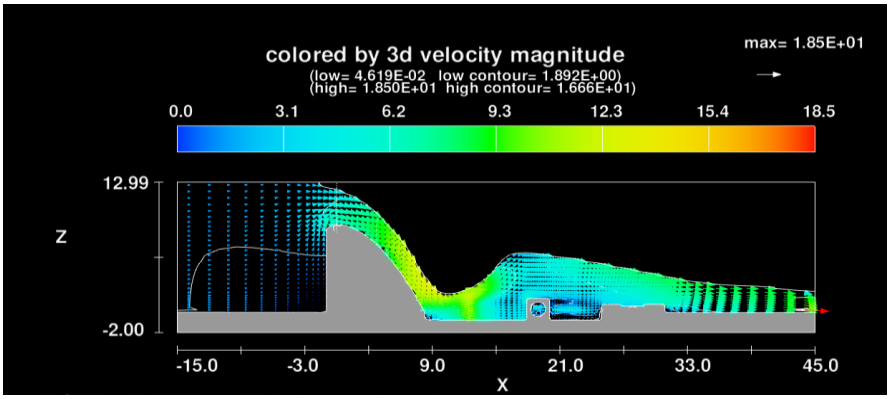

Fig: Model 7 at steady state at final % reduction

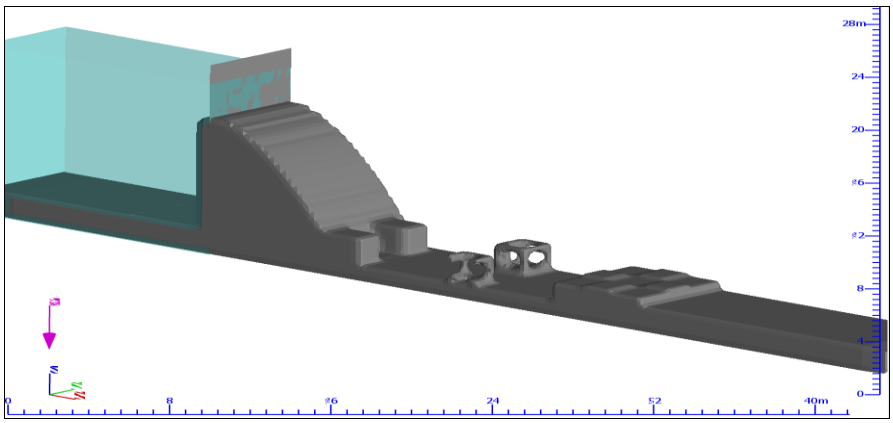

Fig: M2 at 10% reduction in the original length of the stilling basin.

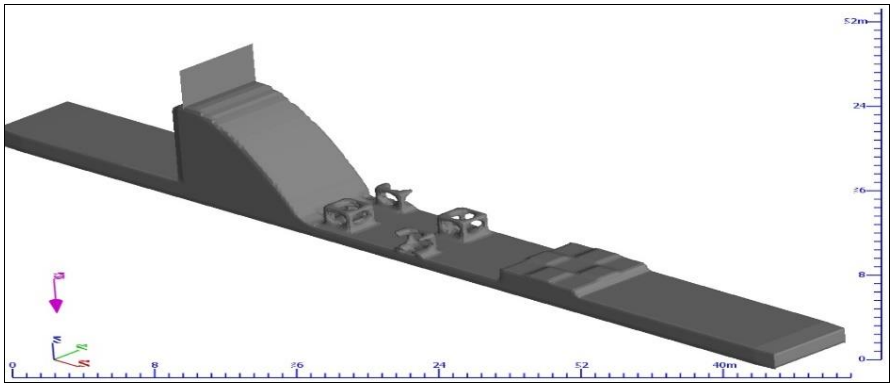

Fig: FAVORing model6 initially.

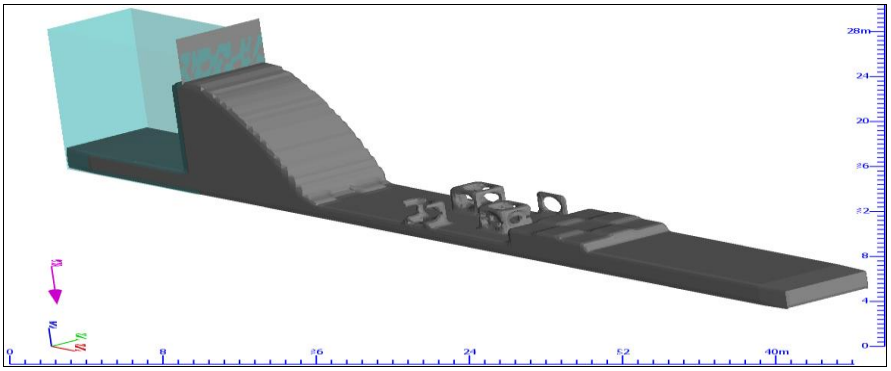

Fig: Favoring model 8 with 5% reduction in length.